The novel leishmanial Copper P-type ATPase plays a vital role in intracellular parasite survival

Rupam Paul[#1], Sourav Banerjee[#1], Samarpita Sen[1], Pratiksha Dubey[2], Anand K Bachhawat[2], Rupak Datta[$1], Arnab Gupta[$1]

[1]Department of Biological Sciences, Indian Institute of Science Education and Research Kolkata, Mohanpur, West Bengal -741246, India

[2]Department of Biological Sciences, Indian Institute of Science Education and Research Mohali, Knowledge city, Sector 81, Manauli, PO, Sahibzada Ajit Singh Nagar, Punjab-140306, India

[#] contributed equally

[$]Correspondence to

Arnab Gupta: arnab.gupta@iiserkol.ac.in; Rupak Datta: rupakdatta@iiserkol.ac.in

Abstract

Copper is essential for all life forms; however in excess it is extremely toxic. Toxic properties of copper are utilized by hosts against various pathogenic invasions. *Leishmania*, in its both free-living and intracellular forms was found to exhibit appreciable tolerance towards copper-stress. To determine the mechanism of copper-stress evasion employed by *Leishmania* we identified and characterized the hitherto unknown Copper-ATPase in *Leishmania major* and determined its role in parasite's survival in host macrophage cells. *L. major* Cu-ATPase, *LmATP7,* exhibits high homology with its orthologues at multiple conserved motifs. In promastigotes, LmATP7 localized to the plasma membrane with a fraction in intracellular puncta. Upon copper treatment, *LmATP7* expression increases few folds. *LmATP7* is capable of complementing copper transport in Cu-ATPase-Δ yeast strain. Promastigotes overexpressing *LmATP7* exhibits higher survival upon copper stress indicating efficacious copper export compared to wild type parasites. We explored macrophage-*Leishmanial* interaction with respect to copper stress subjected by the host upon parasite and the parasite's reciprocating response thereon to evade the stress bit complicated sentence. The Copper-P-type-ATPases ATP7A/7B serves as major copper exporter in eukaryotes that maintain cellular copper levels. We found that *Leishmania* infection, triggers ATP7A upregulation in macrophages. Additionally, as part of host response, ATP7A traffics from trans-Golgi network and transports copper to the endosomal and endolysosomal compartments harbouring the *Leishmania* amastigotes. Finally, we show *LmATP7* overexpression in this parasite, increased amastigote survivability within infected macrophages, establishing its role in combating host-induced copper stress.

Keywords: ATP7, *Leishmania*, Copper, Cu-ATPase, lysosome, ATP7A, host-pathogen interaction

Introduction

Leishmania is a digenetic protozoan belonging to the trypanosomatid group that alternates between sandfly vector and mammalian hosts. They are known to cause a wide spectrum of a tropical human diseases collectively known as leishmaniasis. Severity of the disease depends on the *Leishmania* species and is manifested by a range of symptoms that varies from disfiguring skin lesions to life-threatening infection of the visceral organs.[1] With more than a million new cases and 20,000-30,000 deaths every year, 12 million people are currently affected from about 100 endemic countries imposing a significant threat to the global healthcare system.[2,3] Once the flagellated promastigote form of *Leishmania* enter mammalian host via sand fly bite, they are rapidly phagocytosed by macrophages.[4] Phagocytosis occurs either directly or by engulfment of the parasite-harbouring apoptotic neutrophils followed by transformation from promastigotes into non-flagellated amastigotes in the phagolysosome. Within the acidic phagolysosomes, they continue to proliferate until the cell bursts, leading to the spread of the infection.[5] Inside this compartment *Leishmania* has to withstand a variety of host-induced stress factors including free radicals, lysosomal hydrolases and low pH.[6,7] They are not only equipped to defend against such harsh environment but they can also manipulate host gene expression to their benefit.[8,9,10] Unavailability of a vaccine along with increasing resistance of the existing drugs makes it even more important to understand *Leishmania* physiology and the molecular mechanisms which allow them to thrive inside the host.[11,12]

Copper is an essential micronutrient for biological system. Several enzymes, involved in catalysing biochemical processes, utilize the ability of copper to cycle between cuprous and cupric states. Shuttling between Cu(II) and Cu(I) states can lead to oxidative damage of cells via Fenton like reaction when free copper is available.[13] Organisms have evolved mechanisms where several proteins are involved in tightly regulating the bioavailability of copper.[14] Copper homeostasis, which includes regulating its transport and intercellular distribution, is crucial as excess copper can be detrimental. Copper binding proteins, chaperones, transporters keep intracellular free copper at a very low level in the order of 10^{-18}M.[15]

Various studies have shown that copper plays a key role in host-pathogen interaction. Copper-deficient hosts are more susceptible to several pathogens that include prokaryotes like *Salmonella typhimurium*, *Pasteurella hemolytica* and eukaryotes like *Candida albicans*, *Trypanosoma lewisi*.[16,17,18,19] The bactericidal activity of macrophages and neutrophils is also impaired upon copper deficiency.[20,21] Similarly, copper channelization to the phagosomal compartment of macrophage during *Mycobacterium avium* and *E.coli* infection indicated how hosts tend to utilize copper to fight off intracellular pathogens.[22,23] *E.coli* mutant with a defective copper exporting system showed significantly more susceptibility to copper mediated killing within macrophage.[23]

The P-type Cu-ATPases are involved in removing excess copper from the cell and are one of the key players in maintaining copper homeostasis. In bacteria, CopA and CopB are the Cu-ATPases that carry out this role.[24,25] There is a single Cu-ATPase in lower eukaryotes (non-chordates) referred to as Ccc2p in yeast *Saccharomyeces cerevisiae* or ATP7 in *Drosophila melanogaster* or simply Cu-ATPase.[26] With increased complexity, ATP7A and ATP7B are branched out of ATP7 in higher eukaryotes.[27] In the present study, we

have cloned and functionally characterized a novel copper transporting ATPase (LmATP7) of *Leishmania major* (*LmATP7*) and determined its role in leishmanial survivability in host macrophage. Our study shows for the first time the physiological function of a full-length Cu-ATPase belonging to the kinetoplastida order. Additionally, our study reveals the protective role of LmATP7 in free living promastigotes in copper stress. Further, we also establish that intracellular amastigotes combat host-induced copper stress in lysosomes using LmATP7 that plays a key role in determining its pathogenicity and successful manifestation of infection.

MATERIALS AND METHODS

Reagents were purchased from Sigma-Aldrich (St. Louis, Missouri, United States) unless mentioned specifically. Primers were obtained from GCC biotech (West Bengal, India) and their sequence details are provided in Table S1.

Plasmids and antibodies

Leishmania expression vector (pXG-GFP+) was a generous gift from Dr. Stephen M. Beverley (Washington University Medical School, St. Louis). Mammalian expression vector (pcDNA3.1+) was a kind gift from Dr. Partho Sarothi Ray (IISER Kolkata).

Following are the antibodies were used for experiments: rabbit anti-ATP7A (ab 125137, Abcam, Cambridge, United Kingdom), goat anti-Rab11 (# sc- 6565, Santa Cruz Biotechnology, Dallas, Texas, United States), mouse anti-Rab7 (# sc-376362, Santa Cruz Biotechnology, Dallas, Texas, United States), mouse anti-Lamp1 (DSHB: # H4A3, Iowa City, IA, United States), mouse anti-Lamp2 (DSHB: # H4B4, Iowa City, IA, United States), mouse anti-golgin97 (# A21270, Invitrogen, Carlsbad, California, United States), rabbit anti-calnexin (ab22595, Abcam, Cambridge, United Kingdom), rabbit anti-GFP (# BB-AB0065, Biobharati, Kolkata, India), rabbit anti-GAPDH (# BB-AB0060, BioBharati, Kolkata, India), donkey anti-rabbit IgG (H+L) Alexa Fluor 488 (# A-21206, Invitrogen, Carlsbad, California, United States), donkey anti-goat IgG (H+L) Alexa Fluor 564 (# A-11057, Invitrogen, Carlsbad, California, United States), goat anti-rabbit IgG (H+L) Alexa Fluor Plus 647 (# A32733, Invitrogen, Carlsbad, California, United States), donkey anti-mouse IgG (H+L) Alexa Fluor 568 (# A10037, Invitrogen, Carlsbad, California, United States), goat anti-rabbit IgG-HRP conjugated secondary antibody (# BB-SAB01A, BioBharati, Kolkata, India). The polyclonal antiserum used in this study against LmCA2 has been raised in mouse against recombinant purified protein in our in-house animal facility according to the CPCSEA guidelines and Institutional Animal Ethics Committee approved protocol.

Parasite and mammalian cell culture

The *L. major* strain 5ASKH was a kind gift of Dr. Subrata Adak (IICB, Kolkata). *L. major* promastigotes were cultured in M199 medium (Gibco, Thermo Fisher Scientific, Waltham, Massachusetts, United States)

supplemented with 15% heat-inactivated fetal bovine serum (FBS, Gibco, Thermo Fisher Scientific, Waltham, Massachusetts, United States), 23.5 mM HEPES, 0.2 mM adenine, 150 µg/ml folic acid, 10 µg/ml hemin, 120 U/ml penicillin, 120 µg/ml streptomycin, and 60 µg/ml gentamicin at pH 7.2 and the temperature was maintained at 26°C. The murine macrophage cell line, J774A.1 (obtained from National Center for Cell Sciences, Pune) were grown in Dulbecco's modified Eagle's medium (DMEM, Gibco, Thermo Fisher Scientific, Waltham, Massachusetts, United States) pH 7.4 supplemented with 2 mM L-glutamine, 100 U/ml penicillin, 100 µg/ml streptomycin, and 10% heat-inactivated FBS at 37°C in a humidified atmosphere containing 5% CO2. Cell number was quantified using a hemocytometer.[28]

Infection of macrophages with *L. major* and estimation of intracellular parasite burden

Infection of J774A.1 murine macrophages with late log-phase *L. major* promastigotes was performed as described previously at parasite to macrophage ratio of 30:1.[28] Briefly, the infection was allowed to continue for 12 hours, 24 hours or 30 hours as indicated. For 30 hours of infection, following 12 hours of incubation with J774A.1 macrophages the non- phagocytosed *L. major* promastigotes were removed and the infected macrophage cells were further incubated for 18 hours. After infection, cells were washed and fixed with acetone-methanol (1:1). Anti-fade mounting medium containing DAPI (VectaShield from Vector Laboratories, Burlingame, CA, United States) was used to stain the nuclei of the fixed infected macrophages. Intracellular parasite burden represented as amastigotes/ macrophage cell was quantified by counting the total number of DAPI-stained nuclei of macrophages and *L. major* amastigotes in a field (at least 100 macrophages were counted from triplicate experiments).

Amplification, cloning and sequencing of *LmATP7*

LmATP7 was PCR-amplified using gene-specific primer P15/16 from intron less *Leishmania major* genomic DNA[29] and cDNA and its expression was checked by running the PCR products on 1% agarose gel. Three primer sets P15/16, P15/17 and P18/19 were used for cloning *LmATP7* into pXG-GFP+ (BamHI and EcoRV sites), pcDNA3.1+ (BamHI and EcoRI sites) and yeast expression vector, p416TEF (XbaI and BamHI sites). First two constructs were having C-terminal and N-terminal GFP respectively. All three constructs were confirmed by sequencing.

Generation of *L. major* strain expressing GFP-tagged *LmATP7*

LmATP7-GFP construct or vector control (only pXG-GFP) was transfected into wild type *L. major* promastigotes by electroporation as descried previously to generate the overexpressing *LmATP7* strain.[30] Briefly, 3.6 x 10 7 log phase wild type *L. major* promastigotes were incubated with 30 µg of the DNA construct in electroporation buffer (21mM HEPES, 6mM glucose, 137mM NaCl and 0.7mM NaH_2PO_4; pH 7.4) in a 0.2 cm electroporation cuvette for 10 minutes on ice. Subsequently, electroporation was done in a Bio-Rad Gene

Pulsar apparatus using 475 volts and 550 µF capacitance. The transfected strain was selected and maintained in 100 µg/ml G418 sulphate.

qRT-PCR of Macrophages and *Leishmania* strains specific copper regulators

Total RNA was isolated from uninfected, wild-type *L. major* infected macrophages or from *LmATP7* overexpressing *L. major* strain using TRIzol reagent (Invitrogen, Carlsbad, California, United States). DNA contamination was further removed with DNaseI (Invitrogen, Carlsbad, California, United States) treatment. Verso cDNA synthesis kit (Thermo Fisher Scientific, Waltham, Massachusetts, United States) was used for cDNA preparation from 1 µg of total RNA. Following primers were used for quantification of transcript level of different genes: P1/P2 (*ATP7A*), P3/P4 (*CTR1*), P5/P6 (*CTR2*), P7/P8 (*ATOX1*), P9/P10 (*LmATP7*). Real-time PCR was performed with SYBR green fluorophore (BioRad, Hercules, California, United States) using 7,500 real-time PCR system of Applied Biosystems. The relative transcript level of macrophage specific genes was normalized using wild- type cells as the reference sample and the *β-actin* gene as an endogenous control. In case of LmATP7 mRNA expression, *rRNA45* gene was taken as endogenous control. Amplification of *β-actin* from macrophage and *rRNA45* from *Leishmania* cells was performed using the primer sets P11/P12 and P13/14 respectively.

Immunofluorescence studies and image analysis

Macrophages were seeded at a density of ~2×10^5 cells on glass coverslips and following different experimental steps upto required time points, cells were fixed using acetone: methanol (1:1) for 10 min. Cells were then washed with 1X PBS followed by permeabilization using 0.1% triton-X 100. Both fixation and permeabilization was carried out by keeping it on ice. Cells were then again washed with ice cold 1X PBS, and blocked with 0.2% gelatin for 5 min at room temperature. Incubation with primary antibodies (anti-ATP7A 1:200; anti-Rab11 1:200; anti-Rab7 1:200; anti-Lamp1 1:50 and anti-Lamp2 1:50) was performed for 2 hours at room temperature followed by 1X PBS wash. Cells were reincubated for 1.5 hours at room temperature with either of the following secondary antibodies, goat anti-rabbit Alexa fluor 488 (1:1000) for ATP7A, donkey anti-goat Alexa Fluor 564 (1:1000) for Rab11, goat anti-mouse Alexa fluor 568 (1:1000) for Rab7, Lamp1, Lamp2. Following two 1X PBS washes, coverslips were mounted on glass slides using Fluoroshield™ with DAPI mountant. (#F6057, Sigma-Aldrich, St. Louis, Missouri, United States) and were visualised with Leica SP8 confocal platform using oil immersion 63X objective. IF study was also performed on GFP-*LmATP7* transfected HEK293T cells under basal and 50µM copper treated (2hrs) conditions. Transfection was performed using JetPrime (# 114-07, Polyplus-Transfection, Illkirch-Graffenstaden, France) transfection reagent. Immunostaining was performed using the same above mentioned protocol with primary antibodies, anti-golgin97 (1:200) and anti-calnexin (1:400) and secondary antibodies, donkey anti-mouse Alexa Fluor 568 (1:1000) for golgin97 and goat anti-rabbit Alexa Fluor Plus 647 (1:1000) for calnexin. All images were deconvoluted using Leica Lightning software.

To determine LmATP7 localization in *L. major*, LmATP7-GFP expressing or GFP-only cells were mounted on poly L-lysine coated coverslips, fixed with acetone: methanol (1:1), and permeabilized with 0.1% Triton X-100 at 4ºC. 0.2% gelatin was used to block non-specific binding. Cells were then incubated with either anti-GFP primary antibody or anti-LmCA2 antibody (1:200) for 1.5 hrs. Thereafter cells were washed with ice-cold PBS and incubated with either goat anti-rabbit Alexa Fluor 488 secondary antibody (1:800) or with goat anti-mouse Alexa Fluor 568 secondary antibody (1:600) for 1.5 hrs in the dark. Post-incubation, cells were washed with PBS and embedded in anti-fade mounting medium containing DAPI and visualised with Leica SP8 confocal platform using oil immersion 63X objective.

Bioinformatic analysis of LmATP7

The gene (*LmATP7*) for putative copper-transporting ATPase-like protein was identified from TriTrypDB.[31] The SMART server was used to predict transmembrane domains and Pfam.[32] Clustal Omega was used to generate multiple sequence alignment.[33] Multiple sequence alignment visualisation, analysis and editing was performed using Jalview program.[34] ProtParam was used to determine theoretical molecular weight and isoelectric point.[35]

Homology modelling and structural validation

We modelled the three Heavy Metal Binding Domains (HM) of *Leishmania* P-type ATPase copper transporter. The sequence of the three domains that are used for homology modelling include as follows:

HM1:

TLNVFGTTCRGCAQHVQENLMTLEGVHSVSVDLDAQLAEVDVDATDAATEFRIEKKMVSMGY

HM2:

LLIEGMSCTSCAARIEAKLKQLKGVLGASVNFSAMSGQVLHNPALAPLPKVVSCVADMS

HM3:

DGEQPQEGECKCPTNLQAVPVHVGSVMSGYEHRLVVLGMSCASCAARIEHRLRQMPTVLNCTVSF VTGTAV

All these three contain the putative copper binding motif (CXXC), which is thought to be responsible for copper transport. In order to provide a possible structure we performed homology modelling followed by Molecular Dynamics simulations. There is no experimentally resolved 3D structure for the metal binding domains of *Leishmania* ATP7. In order to find the most similar sequence whose structure is known (template) to each of the target sequence, sequence similarity search was performed on the BLASTp online server (http://blast.ncbi.nlm.nih.gov) which were subsequently used as templates for homology modelling performed using the Modeller 9.25 program[36]. This yielded the initial structural guesses for the HMs. The best model was selected with regard to the best Discrete Optimization Protein Energy (DOPE) score.[37] Initially each of the aforementioned best models was solvated by ~40000 TIP3P water molecules in a box of dimension 80x80x80 Å3.[38] The physiological concentration (150 mM) of Na+ and Cl- ions along with extra ions were

used to neutralize the system. These were subsequently energy minimized using the steepest descent method for 10000 steps, followed by heating it to 300K in 200 ps using Berendsen thermostat and barostat with coupling constant of 0.6 ps. Restraints of 25 kcal/mol/Å2 were applied on heavy atoms during the heating process. Thereafter, equilibration was carried out for 2 ns at constant temperature (300 K) and pressure (1 bar) without any restraints using the same thermostat and barostat with coupling constants of 0.2 ps each. The last 100 ps of NPT simulation was used to calculate the average volume the same, which was used in the final 1000 ns unrestrained NPT equilibration using the Velocity-Rescale thermostat[39] and a Parrinello-Rahman barostat[40] with coupling constant of 0.2 ps. During the simulation, LINCS algorithm was used to constrain all the bonds and Particle Mesh Ewald (PME) method[41] was used for electrostatics. The distance cut-offs for the van der Waals (vdW) and electrostatic long-range interaction was kept at 10 Å. The time step for each simulation was taken to be 2 fs. All of the simulations were performed using molecular dynamics software GROMACS 2019.4[42] with parameters from the AMBER99SB force field.[43]

Immunoblotting

Transfected HEK293T cells were washed twice with ice-cold 1X PBS and scrapped off into a centrifuge tube. Following centrifugation at 3,000 rpm for 5 min, the cell pellet was suspended in RIPA lysis buffer (composition: 10mM Tris-Cl pH 8.0, 1mM EDTA, 0.5mM EGTA, 1.0% Triton X-100, 0.1% sodium deoxycholate, 0.1% sodium dodecyl sulphate, 140mM NaCl, 1X protease cocktail inhibitor). After a brief incubation on ice, the cell solution was sonicated (3 pulses, 5 secs and 100mA) to prepare whole cell lysate. Bradford reagent (# B6916-500ML, Sigma-Aldrich, St. Louis, Missouri, United States) was used for protein estimation following manufacturer's protocol. Sample preparation was done with 30µg of protein and 4X loading buffer (composition: Tris-Cl pH 6.81, 4% SDS, 10% β-ME, 20% glycerol, 0.02% bromophenol blue, urea 8M). The samples were subjected to sodium dodecyl sulphate-polyacrylamide gel electrophoresis (SDS-PAGE) followed by wet transfer onto nitrocellulose membrane (1620112, BioRad, Hercules, California, United States). Both Anti-GFP and anti-GAPDH antibodies were used at a dilution of 1:3000. HRP-conjugated goat anti-rabbit secondary antibody was used at a dilution of 1:5000. The blots were developed using by ECL developer (170-5060/1705062 BioRad, Hercules, California, United States) in chemiluminescence by Chemi Doc (BioRad, Hercules, California, United States).

Strains, media, growth conditions for yeast complementation assay

For yeast complementation studies, *Saccharomyces cerevisiae* BY4742 (wild-type) strain (*MATα his3Δ1 leu2Δ0 lys2Δ0 ura3Δ0*) and an *S. cerevisiae* strain carrying a CCC2 deletion (ccc2Δ) in the BY4742 background purchased from Euroscarf (Oberursel, Germany) were used. YPD (yeast extract, peptone, and dextrose) medium was used for routinely maintaining both wild-type and deletion strains. For complementation assay, synthetic defined (SD) minimal media containing YNB (yeast nitrogen base), ammonium sulfate, and dextrose supplemented with histidine, leucine, lysine, and methionine (80 mg/liter)

were used. Yeast transformations were carried out using lithium acetate method.[44] Human *ATP7B* mRNA was cloned in p416TEF vector (as a positive control) and confirmed by sequencing. *LmATP7* and human *ATP7B* constructs along with empty vector p416TEF were used to transform wild-type (Wt) and ccc2Δ strains. Yeast transformants were selected and maintained on SD medium without uracil (SD-Ura) at 30°C. p416TEF vector contains URA3 selection marker allowing growth in absence of uracil. Wild-type strain was transformed with empty vector to allow its growth on SD-Ura.

In Vivo Functional Complementation assay in *S. cerevisiae* by dilution spotting

Yeast transformants were grown overnight at 30°C with shaking at 200 rpm in SD-Ura medium. Primary culture was used to inoculate secondary culture in the same selective medium and allowed to grow at 30°C till OD_{600} reached about 0.6. The cells were centrifuged, washed and diluted in sterile water at $OD_{600} = 0.2$. Serial dilutions were then made with sterile water ($OD_{600} = 0.2$, 0.02, 0.002, 0.0002) and 10 µl of cell suspension from each were spotted on plates containing SD-Ura medium with or without 250µM iron chelator, Ferrozine (Sisco Research Laboratories, Mumbai, India). Plates were incubated at 30°C for 3 days and photographs were taken.

Statistical analysis

For statistical analysis and plotting, ggplot2 package was used in R v-3.4.0.[45,46] All statistical analyses were performed by Student's t test or by one-way ANOVA calculator. The results were represented as mean ± SD from minimum three independent experiments. P values of ≤ .05 were considered statistically significant, and levels of statistical significance were indicated as follows: *P ≤ .05, ** P≤ .01, *** P ≤.001, ****P≤ .0001.

Results

***Leishmania* genome encodes and expresses P-type Copper ATPase**

Copper has been conventionally used as a chemotherapeutic agent against parasitic infections.[22,23,47] To explore if lethality could be induced in *Leishmania* parasites, we tested survivability of the parasite in growth media supplemented with copper in a range between 0-500µM for 24 hours. Corroborating with copper induced toxicity, both free living promastigotes as well as intracellular amastigotes showed a gradual decline of survivability with increasing copper concentration, with around a third of the parasites surviving at 500µM as compared to controls (Figure 1A,B). However, given that the internal copper in the parasite is maintained at an extremely low level (~0.001-0.002 ppm as measured in promastigotes using ICP-OES), the survivability trend indicated that *L. major* exhibits copper resistance or tolerance to an appreciable extent. We argue that an efficient copper handling machinery is present in the parasite that confers its survivability in elevated non-physiological copper.

We attempted to identify if *Leishmania* genome encodes for any Copper exporter that might be key for its survival in copper stress within the macrophagic lysosomes during infection or in artificial experimental

condition as tested in the previous section (as shown in Figure 1A,B). We identified a putative copper transporting P-type ATPase (*LmATP7*) in the genome of *Leishmania major* from the kinetoplastids informatics resources, TriTrypDB. It is predicted to have three heavy metal-binding domains (Pfam PF00430) in its N-terminal region, each containing the characteristic Cu^+ binding motif, CXXC. It has the highly conserved TGE sequence in the actuator (A) domain and DKTGT sequence in the phosphorylation (P) domain. Both A and P regions are contained within the E1-E2 ATPase domain (Pfam PF00122), where E1 and E2 are the two cation binding states (Figure 2A). The catalytic activity of Cu ATPases is exhibited through phosphorylation and dephosphorylation of Asp residue in the conserved DKTGT motif. LmATP7 is also comprised of a hydrolase region (Pfam PF00702) containing TGDN and GXGXND conserved motifs in the ATP binding site of the nucleotide binding domain and the SXHP motif whose mutation in human orthologue ATP7B (His1069Gln) is the most frequent contributor to Wilson Disease in the Caucasian population (Figure 2B). The SMART server predicted nine transmembrane domains (TMDs) in LmATP7, which is similar to the predicted TMDs in *Trypanosoma congolense*.[48] To date, no more than eight TMDs have been shown experimentally in Cu-ATPases across species. The extra TMD could be unique to some species of the kinetoplastida. LmATP7 contains copper coordinating CPC motif in the seventh TMD that is conserved in the IB P-type ATPase family. The genomic DNA and RNA of *Leishmania major* were isolated and amplified (cDNA from RNA) using primers designed to amplify the *LmATP7*. Gel electrophoresis data showed a fragment of about 3500bp for both genomic DNA and cDNA indicating its transcriptional expression which was subsequently confirmed by Sanger sequencing (Figure 2C). The sequencing result revealed a DNA fragment of 3492bp, which is identical to the length of the putative copper-transporting ATPase-like protein encoding gene [*Leishmania major* strain Friedlin, GeneID 5654633]. Although both encoded identical amino acid sequence (1163 in length), *LmATP7* gene from our *L. major* strain 5ASKH differed in six nucleotides from the sequence of Friedlin strain. Both gene and mRNA sequence of *LmATP7* are submitted to the GenBank (accession numbers MW261996 and MW261995 respectively).

N-terminus Copper binding motifs of LmATP7 share high homology with mammalian Cu-ATPases

PIB-ATPases are heavy-metal-transporting ATPases characterized by the unique presence of Heavy metal (HM) binding sites at the luminal N-terminal domain. We detected three putative HM motifs with the conserved Cys-X-X-Cys motif in LmATP7. The sequence of the three domains that are used for homology modelling are included in the Materials and method section. Based on E-value of alignment (0.65E-04) the template that was chosen for homology modelling of HM1 was *Bacillus subtilis* CopA (PDB ID: 1OPZ) with the percentage sequence identity between the template and the model normalized by the lengths of the alignment being 30. The modelled structure with the lowest DOPE score of -4818.916016 was selected for further validations and simulation studies (Figure 2D).

Initially HM2 and HM3 were modelled together since they are in close proximity to one another and hence thought to have evolutionarily co-evolved as compared to HM1 which is sequence-wise farther away. Based

on lowest E-value of alignment (0.48E-10), a NMR structure of soluble region of P-type ATPase CopA from *Bacillus subtilis* (PDB ID: 1P6T) was the best template for these two domains combined together. Both the human copper ATPases (ATP7A or ATP7B) lost out on homology modelling both in terms of sequence similarity (29 %) as well as E-value of alignment (0.14E-08). The modelled structure with the lowest DOPE score of -12928.405273 was selected for validation and simulation studies (Figure 2D).

Surprisingly, when HM2 and HM3 are modelled separately, they show a better homology modelling with human copper ATPases as compared to bacterial ones. For HM2, based on the lowest E value of alignment (0.32E-06) the template which was found suitable for homology modelling was the solution structure of the metal binding domain 4 of human ATP7B (PDB ID: 2ROP) with the percentage sequence identity between the template and the model normalized by the lengths of the alignment being 36. Though there was also a significant percentage sequence identity (45 %) between our model and *Bacillus subtilis* CopA (PDB ID: 1OPZ) and an even lower E value of 0.51E-07, it was rejected based on a huge mismatch in the DOPE per residue score vs alignment position graph between the CopA template and the modelled structure of *Leishmania* HM2 ((Figure S1). The modelled structure with a lowest DOPE score of -4788.835449 was selected for validations and simulation studies (Figure 2D).

For HM3, based on the lowest E value of alignment (0.68E-04) the template which was found suitable for homology modelling was the solution structure of the metal binding domains 6 of human ATP7A (PDB ID: 1YJV) with the percentage sequence identity between the template and the model normalized by the lengths of the alignment being 46. Though there was also a significant percentage sequence identity (49 %) between our model and *Bacillus subtilis* CopA (PDB ID: 1OPZ) and an even lower value E-value of 0.32E-05, it was rejected based on a huge mismatch in the DOPE per residue score vs alignment position graph between the CopA template and the modelled structure of *Leishmania* HM3 (Figure S1). The modelled structure with a lowest DOPE score of -5403.311035 was selected for validations and simulation studies (Figure 2D).

The above mentioned four models with the lowest DOPE scores obtained through homology modelling were first equilibrated as mentioned in Materials and Methods section followed by a final 1000 ns unrestrained NPT equilibration. The final structures were then obtained by averaging out the last 100 ns of the production runs (Figure 2D).

Intracellular localization of LmATP7 in the promastigote and mammalian cells is consistent with other characterized orthologues

The human orthologues ATP7A and ATP7B localizes at the trans-Golgi network and traffics in vesicles to plasma membrane upon copper treatment. To determine if LmATP7 localizes in plasma membrane of *Leishmania*, we cloned and we expressed GFP-*LmATP7* in promastigotes (Figure S2; Figure 3A) and co-labelled it with a cell surface marker LmCA2 (Carbonic anhydrase 2). Partial colocalization between the two proteins were observed; with a fraction of intracellular puncta of GFP-LmATP7 that did not colocalize (Figure

3B,C). We hypothesize that this unascertained intracellular GFP signal probably represents Golgi and endosome-residing LmATP7.

Given the size of the parasite, it is difficult to resolve if LmATP7 is capable of trafficking in response to copper in its natural cellular environment, i.e., the *Leishmania* amastigote or the promastigote. In higher eukaryotes, apart from transporting copper to copper-dependent enzymes, Cu-ATPases traffic out of Golgi to remove excess copper from the cell.[49] The idea of transiently expressing GFP tagged LmATP7 in HEK293T cell line was to find out if LmATP7 exhibits copper responsive trafficking. LmATP7 expressed in HEK293T was stable (Figure 3D). Immunofluorescence (IF) study revealed that GFP-LmATP7 localizes in the trans-Golgi network along with endoplasmic reticulum (ER) (Figure 3E). ER localization of GFP-LmATP7 can be attributed to its overexpression or it being expressed in a foreign organism is sub-optimally folded. To check whether GFP-LmATP7 traffics out of Golgi in excess copper as observed for mammalian Cu-ATPases, transfected HEK cells were treated with 50µM $CuCl_2$ for 2 hours. Upon copper treatment, we observed vesicularization of GFP-LmATP7, but to a much lower extent as compared to ATP7A vesicularization (Figure 3E and Figure S3). This lower copper-responsive trafficking could be attributed to (a) LmATP7 lack three of the six copper binding domains as in ATP7A/7B that has been shown to be critical for Golgi exit and vesicularization[50,51] and (b) lipid bilayer composition embedding the Copper ATPase of Leishmanial membranes are probably distinct and different from its mammalian counterparts, affecting its vesicularization. However, finding out its localization within *Leishmania major* will provide more information about its behaviour with respect to trafficking.

LmATP7 is a *bona fide* copper transporter

As a homeostatic response, copper treatment upregulates ATP7A in mammalian cells.[52] To determine if copper has a role on LmATP7 regulation in *Leishmania*, we treated *Leishmania* promastigotes with 50µM copper for 2 hours, and measures the mRNA levels. We observed an 8 fold upregulation under copper treatment indicating its possible role in maintaining copper homeostasis (Figure 4A).

To determine if LmATP7 is a *bona fide* copper ATPase, we used a functional assay that has been developed for human P-type Cu-ATPases, ATP7A/B and its mutants. This assay is based on functional complementation of the CCC2 deletion mutant (*ccc2Δ*) of the yeast *Saccharomyces cerevisiae*.[53] Ccc2p, the P-type ATPase copper transporter of *S. cerevisiae* transports copper to the plasma membrane oxidase Fet3p, which then works with a high affinity iron importer Ftr1p to import iron from the medium. In the yeast deletion mutant *ccc2Δ*, copper is not incorporated into Fet3p leading to deficiency in high affinity iron uptake. In iron-sufficient medium, the *ccc2Δ* can grow well owing to the ability of low affinity iron uptake systems to supply iron to the cells. However, in iron limited medium, this mutant fails to grow as Fet3p-Ftr1p, which becomes essential under these conditions, is non-functional. ATP7B, in previous studies, has been shown to complement the *ccc2Δ* mutation allowing the mutant cells to grow in iron-limited medium, establishing this as a convenient functional assay for P-type Cu-ATPases.

The *cerevisiae ccc2Δ* mutant was accordingly transformed with plasmids carrying either the *LmATP7* expressed downstream of the strong TEF promoter in a single copy centromeric vector (p416TEF-*LmATP7*) or the empty vector pTEF416 or the human *ATP7B* that was similarly expressed as a positive control (p416TEF-*ATP7B*). The transformants that appeared were evaluated for growth in iron deficient and iron-sufficient (control) media by serial dilution assays. We observed that expression of LmATP7 in *ccc2Δ* was able to complement the mutation restoring their growth in iron-limited medium. In contrast, the cells bearing the vector control failed to grow. The p416TEF-*ATP7B* construct complemented more strongly as compared to LmATP7 and may reflect either differences in expression of the two genes in yeast, or possible differences in functional efficiency. Importantly, LmATP7 showed complementation indicating that this leishmanial protein was able to functionally complement *CCC2* in vivo (Figure 4B). Hence *LmATP7* can be functionally ascertained as the IB P-type copper transporting ATPase in *Leishmania major*.

Overexpression of LmATP7 imparts copper tolerance to promastigotes

Since we have ectopically expressed and established LmATP7 as a Cu-ATPase in yeast, we now investigated if the protein is capable of regulating copper homeostasis in *Leishmania*.

L. major promastigotes, stably expressing GFP-LmATP7 or not (GFP-only or WT) were grown under normal and increased copper conditions for 24 hours (0- 500uM). Higher expression of *LmATP7* was confirmed in promastigote population that stably overexpressed *GFP-LmATP7* (Figure 5A). All three promastigote populations experienced reduced growth with increased copper in the medium, indicating cytotoxic effects of excess copper. At 500uM concentration of external copper, wild-type and GFP only expressing promastigotes count were lower than the initial seeded number indicating cell death. Interestingly, LmATP7 overexpressing promastigotes count was significantly high than the controls at such heightened copper level (Figure 5B). Although its growth decreased gradually with increasing copper conditions, it consistently maintained a higher growth rate than the controls. This indicates an enhanced copper export activity in LmATP7 overexpressed promastigotes, allowing a relatively better internal copper regulation and reduced cytotoxic effects. Both the controls were also able to survive and maintain their growth to some extent under excess external copper, probably owing to their endogenously expressed LmATP7. At extremely high copper, endogenous LmATP7 seemed to be insufficient to maintain internal copper homeostasis, leading to tremendous growth retardation and cell death. The results provided the first evidence of the role of the newly characterized leishmanial Cu-ATPase, LmATP7, in copper tolerance.

Macrophages channelizes copper to intracellular compartments harbouring *Leishmania* amastigotes

To further delineate the role of LmATP7 in a physiological condition, we explored host-*Leishmainia* interaction with respect to copper stress subjected by the host upon parasite and the parasite's reciprocating response thereon to evade the stress. At the outset, we examined alterations of macrophage transcripts levels (if any) of the key genes of copper homeostatic pathway during *Leishmania* infection. J774A.1 macrophages

were infected with *L. major* promastigotes and infection was confirmed and measured by counting the nuclei of amastigotes in the macrophage. Transcripts of Cu-ATPase, *ATP7A*, copper transporters, *CTR1*, *CTR2* and copper chaperon, *ATOX1* was measured 12 hours and 30 hours post infection. Interestingly, all four genes were downregulated at the shorter post infection time-point; however, at 30 hours post infection, *ATP7A* exhibited ~1.8X upregulation. Other transcripts also exhibited modest upregulations (Figure 6A). The results suggested that host copper uptake and utilization is downregulated during early stages of infection. However, the host exerts its copper mediated response at a later stage with upregulation of *ATP7A*, *CTR1* and *CTR2*.

To export excess copper, ATP7A traffics to vesicles out of TGN (Trans-Golgi network) when cells are treated with high copper.[54,55,56] Hence, as a function of copper transport, we probed intracellular localization and TGN exit of ATP7A at 24 hours post- *Leishmania* infection. The time point fits between the heightened parasite response and heightened host response. Interestingly, ATP7A traffics out of Golgi in vesicles in *L. major* infected macrophages. ATP7A in uninfected macrophages remained clustered at the Golgi (Figure S3). This observation is consistent with our finding that ATP7A traffics in vesicles out of TGN in response to copper and LPS (Figure S3).

Since, we determined that *Leishmania*, post-internalization, localizes in the macrophages throughout the endosomal pathway, we determined the nature of the ATP7A positive compartment that harbours these amastigote parasite. To scan the entire endocytic pathway we measured percentage of colocalization between ATP7A, the intra-macrophagic amastigote nuclei and the endosomal/endo-lysosomal markers, Rab11 (recycling endosome), Rab7 (late endosome) and Lamp1/2 (endo-lysosome). We noticed that colocalized ATP7A-amastigote nuclei distributes throughout the endosomal pathway (Figure 6B); with highest localization at the Lamp1 positive compartments (Figure 6C).

Leishmania overexpressing LmATP7 shows increased amastigote survivability

It is now obvious that as a host response, the macrophage deploys the copper transport machinery to exert stress on the intracellular parasites. We argue that *Leishmania* overexpressing LmATP7 would handle copper stress more efficiently brought-upon by the host macrophage as compared to wild-type parasites.

Stable lines of *L. major* expressing GFP-LmATP7 was generated and were subsequently used to infect J774A.1 macrophages under normal and increased copper conditions. Empty vector (pXG-GFP+) expressing and wild type promastigotes were used as controls. Corroborating with our hypothesis, we found that *L. major* amastigotes overexpressing GFP-LmATP7 were significantly higher in abundance as compared to both the controls (Figure 7A). This increase was consistent both at normal and copper-treated conditions. Amastigote count went down with increasing copper concentration indicating an antagonistic role of copper against all three amastigote populations (Figure S4). When overexpressed, LmATP7 by exporting copper from *Leishmania*, provided increased survivability to the amastigotes (Figure 7B). Previous studies showed bactericidal activity is promoted by intracellular bio-available copper in macrophages which was further facilitated by external copper treatment.[23] We observed a similar phenotype of reduced intracellular

amastigotes with increasing copper level. As illustrated in Figure 6B, even under physiological copper condition, activated macrophages increase copper import and partially channel copper via ATP7A towards the endo-lysosomal compartments. LmATP7 overexpressed protein was probably more efficient in removing excess copper from the *Leishmania* cells as compared to the endogenously expressed one resulting in higher amastigote per macrophage cell. Overall, the experimental data revealed the importance of LmATP7 in neutralizing toxic levels of copper from the host on *Leishmania* amastigotes. It improved the survivability of the amastigotes, thereby, increasing the parasite burden within the macrophage host. The model (Figure 8) illustrates the interaction of the host and parasite copper-ATPases in the infected macrophage.

Discussion

Host-parasite interaction is a rapidly evolving field. Host-parasite interaction has served as apt example of 'red queen hypothesis of winner less antagonistic coevolution'.[57] Host and the parasite co-evolves where parasites adapt to neutralize any response that is employed by the host to evade parasite invasion. Macrophage cells, being the sentinel of our immune system play pivotal role in eliminating different pathogenic infections.[58] However, *Leishmania* parasites specifically infect and survive within these cells. Macrophages have been shown to express the key copper-homeostatic genes. Further, it has been demonstrated that in the case of pathogenic yeast, *Candida* sp. infection, macrophage deploys the copper ATPase, ATP7A to exert copper-mediated toxicity over the pathogen.[59] However, there is no such report which addresses if macrophages being the host to *Leishmania* tries to combat the infection using similar mechanism or if so, then how the parasite escapes such host-induced stress. In this context, we have identified and characterized the Cu-ATPase, LmATP7 for the first time in the kinetoplastid parasite genus, *Leishmania*. Furthermore, using the well-established macrophage- *Leishmania* infection model system we found that there is a reciprocal interaction between the copper ATPases of the host and the parasite that determines the fate of parasite survivability and well-being of the antagonistic pair.

We observed that upon increasing concentration of copper treatment wild-type *L. major* promastigotes could overcome the toxic effect of this metal ion. This observation is particularly interesting since the other known bacterial pathogens are reported to be susceptible towards copper concentration as low as 20 µM.[23] Although at 50uM and higher external Cu treatment, there was drop in parasite count, *Leishmania* could maintain its population appreciably at a very high Cu concentration of 500 µM. We noticed a similar survival trend even in the intracellular amastigotes in these copper conditions. These two exciting observations collectively suggest that there must be an efficient copper homeostasis mechanism within *Leishmania* which is expressed both in its extracellular promastigote form as well as in its infectious amastigote stage.

Importance of copper in kinetoplastid parasites is unknown. Though the Cytochrome C oxidase complex (that is known to bind copper) has been identified in *Leishmania* and its component Ldp27 has been shown to be crucial in amastigote survival, no information is available about role of copper in the secretory pathway.[60] Although role of iron has been extensively studied in kinetoplastid parasites; there has been limiting efforts to

understand the role of copper in their survival or pathogenicity. Mammalian Copper ATPase, ATP7A carries out two primary functions. Firstly, it transports copper to enzymes that require the metal as a co-factor for maturation, e.g., Dopamine-β-hydroxylase and tyrosinase. Secondly, upon copper excess in the cell, ATP7A traffics in vesicles to export out the excess copper.[54] In a polarized epithelial cell, as in intestinal enterocytes, ATP7A transports copper through the basolateral surface (blood-side) that is further picked-up in the serum by copper-sequestrating proteins, e.g., albumin. However, in unpolarised cells, e.g., macrophages and fibroblasts, the copper transporter vascularizes upon excess copper and localizes at the lysosomes and exports copper by triggering the lysosomal exocytosis pathway.[56,61,62] Thus, it would be interesting to determine if *Leishmania* copper ATPase carries out the dual function of copper detoxification as well as copper transport to the secretory pathway as done by its mammalian counterparts, ATP7A and ATP7B.

Recently it has been demonstrated that *Trypanosome* genome codes for a copper-ATPase.[48] We identified a putative *Leishmania* specific P-type ATPase with three predicted N-terminal copper binding motifs and nine transmembrane domains. It is worth mentioning that lower order eukaryotes carry a single copper-ATPase; however with the advent of cellular apico-basal polarity and increasing tissue complexity in higher organisms, this copper-ATPase branched out into two homologues ATP7A and ATP7B. Our in depth bioinformatics analysis depicted this putative ATPase as a copper transporter which was further confirmed with the yeast complementation study. Like its other protozoan counterpart, *Plasmodium berghei* and *Toxoplasma gondii*,[63] the LmATP7 is present both in endosomal compartments as well as in plasma membrane. It is well-known that mammalian CuATPases, in response to high levels of copper, relocalizes to the vesicles that eventually fuse with the plasma membrane to remove excess copper from the cell.[54,55] Interestingly, upon expressing LmATP7 in mammalian cells we could find a low level of trafficking of this protein from TGN to vesicles upon a brief exposure to copper. Though *Leishmania* is far removed from mammals, copper-responsive trafficking of LmATP7 in mammalian cells confirms the maintenance of its primary function as a copper exporter.

To inflict a copper induced stress on *Leishmania*, ATP7A of the macrophage traffics to transport copper to compartments that harbour the parasites. Amastigotes overexpressing LmATP7 exhibit a significant higher colonization in the macrophages as compared to the wild-type controls, further establishing the role of LmATP7 in combating host copper stress. A similar trend of higher parasite survivability of the LmATP7-overexpressing strain was observed upon increasing copper treatment of the macrophages harbouring the amastigotes. It is worth mentioning that at least up to 200 µM Cu treatment the parasite burden in LmATP7 overexpression strain infected macrophages was ≥ 3 (amastigotes/ macrophage cell) which is about two fold higher than the parasite burden in either wild-type *Leishmania* or vector control infected macrophages.

Although it has been reported that several intracellular pathogens try to arrest the phagosome maturation process in the host macrophage cells to avoid transport to lysosomes, *Leishmania* is exceptional since it prefers to reside within the endolysosomal and the phagolysosomal compartment.[5,64] There are numerous reports that demonstrate macrophage cells can actively accumulate and compartmentalize copper

in response to developing potential anti-microbial activities.[23,65] In fact, it has been shown that copper concentration within phagolysosomal compartment of macrophages increases significantly when infected with *Mycobacteria*.[22] This might be a crucial step towards parasite killing, since under the acidic environment of the phagolysosome, copper can react with the readily available reactive oxygen and nitrogen species to exert its toxicity.[23,66] Hence, it will be interesting to determine if macrophage cells also utilize copper in a similar fashion to kill *Leishmania* and the reciprocal response of the parasite, if any. Along this line, our observation of parasite mediated downregulation of macrophage *ATP7A*, *CTR1*, *CTR2* as well as *ATOX1* at early time point, i.e., 12 hrs post infection with *L. major* implicates the same for the first time. In the putative series of event, we argue that as a host response, the macrophage upregulates ATP7A followed by its copper transport to the endosomal pathway harbouring the parasite. Subsequently, the parasite responds by upregulating the copper ATPase, LmATP7 to alleviate the host-induced copper stress and eventually survives inside the macrophage.

Recently, it has been shown that *Leishmania* hijacks host regulatory pathways that control expression of a phagolysosomal iron transporter so that it can effectively acquire iron for its survival by increasing the concentration of this metal ion within phagolysosomes.[28] This is certainly a parasite mediated remodelling of host machineries. However, our study shows that unlike in iron homeostasis, host macrophages tries to concentrate copper within *Leishmania* containing phagolysosomal compartment to kill the pathogen. To counteract this toxic effect the pathogen has armoured themselves with the CuATPase, LmATP7. Hence, it will be extremely important to identify the underlying mechanisms behind the parasite mediated downregulation of host's Cu utilization proteins as well as how LmATP7 could be targeted to develop novel anti-leishmanial drug.

Acknowledgments

This work was supported by DBT-Wellcome Trust India Alliance Fellowship (IA/I/16/1/502369) and Early Career Research Award (ECR/2015/000220) from SERB, Department of Science and Technology (DST), Government of India and IISER K intramural funding to AG and Department of Biotechnology (DBT) and Department of Science and Technology (DST) grants BT/PR21170/MED/29/1109/2016 and EMR/2017/004506, respectively to RD. RP and SB was supported by Pre-doctoral fellowship from Council of Scientific and Industrial Research and DST INSPIRE, India, respectively. SS was supported by KVPY fellowship, India. We thank Moulinath Acharya (NIBMG) and Sudipta Chakraborty (NIBMG) for helping us with Real-time PCR

Author contributions:

AG, RD, RP, SB and SS designed the experiments and wrote the manuscript. RP, SB, SS and PD did the experiments and analysed the data. PD and AKB helped with yeast complementation experiments. SS did the homology modelling. All authors reviewed the results and approved the final version of the manuscript.

The authors declare no competing financial interests.

Bibliography

1. Burza S, Croft SL, Boelaert M. Leishmaniasis. *The Lancet* 2018; doi:10.1016/S0140-6736(18)31204-2.
2. Okwor I, Uzonna J. Social and economic burden of human leishmaniasis. *American Journal of Tropical Medicine and Hygiene* 2016; doi:10.4269/ajtmh.15-0408.
3. Alvar J, Vélez ID, Bern C, Herrero M, Desjeux P, Jorge Cano, Jean Jannin, Margriet den Boer. Leishmaniasis worldwide and global estimates of its incidence. *PLoS ONE* 2012; doi:10.1371/journal.pone.0035671.
4. Peters NC, Egen JG, Secundino N, Debrabant A, Kimblin N, Kamhawi S, Lawyer P, Fay MP, Germain RN, Sacks D. In vivo imaging reveals an essential role for neutrophils in leishmaniasis transmitted by sand flies. *Science* 2008;Aug 15;321(5891):970-4. doi: 10.1126/science.1159194. Erratum in: *Science* 2008 Dec 12;322(5908):1634.
5. Chang KP, Dwyer DM. Leishmania donovani: Hamster macrophage interactions in vitro: Cell entry, intracellular survival, and multiplication of amastigotes*. *J. Exp. Med* 1978; doi:10.1084/jem.147.2.515.
6. Haas A. The phagosome: Compartment with a license to kill. *Traffic* 2007; doi:10.1111/j.1600-0854.2006.00531.x.
7. Thi EP, Lambertz U, Reiner NE. Sleeping with the enemy: How intracellular pathogens cope with a macrophage lifestyle. *PLoS Pathog* 2012; doi:10.1371/journal.ppat.1002551.
8. Gregory DJ, Sladek R, Olivier M, Matlashewski G. Comparison of the effects of Leishmania major or Leishmania donovani infection on macrophage gene expression. *Infect. Immun* 2008; doi:10.1128/IAI.01320-07.
9. Beverley SM. Hijacking the cell: Parasites in the driver's seat. *Cell* 1996; doi:10.1016/S0092-8674(00)81984-4.
10. Carrera L, Gazzinelli RT, Badolato R, Hieny S, Muller W, Kuhn R, Sacks DL. Leishmania promastigotes selectively inhibit interleukin 12 induction in bone marrow-derived macrophages from susceptible and resistant mice. *J Exp Med* 1996; Feb 1;183(2):515-26. doi: 10.1084/jem.183.2.515.
11. Croft SL, Sundar S, Fairlamb AH. Drug resistance in leishmaniasis. *Clinical Microbiology Reviews* 2006; doi:10.1128/CMR.19.1.111-126.2006.
12. Sundar S, Jaya J. Liposomal amphotericin B and leishmaniasis: Dose and response. *J. Glob. Infect. Dis.* 2010; doi:10.4103/0974-777x.62886.
13. Festa RA, Thiele DJ. Copper: An essential metal in biology. *Current Biology* 2011; doi:10.1016/j.cub.2011.09.040.
14. Hodgkinson V, Petris MJ. Copper homeostasis at the host-pathogen interface. *Journal of Biological Chemistry* 2012; doi:10.1074/jbc.R111.316406.
15. Nevitt T, Öhrvik H, Thiele DJ. Charting the travels of copper in eukaryotes from yeast to mammals.

Biochimica et Biophysica Acta - Molecular Cell Research 2012; doi:10.1016/j.bbamcr.2012.02.011.

16. Newberne PM, Hunt CE, Young VR. The role of diet and the reticuloendothelial system in the response of rats to Salmonella typhilmurium infection. *Br J Exp Pathol* 1968; Oct;49(5):448-57.
17. Jones DG, Suttle NF. The effect of copper deficiency on the resistance of mice to infection with Pasteurella haemolytica. *J. Comp. Pathol* 1983; doi:10.1016/0021-9975(83)90052-X.
18. Jones DG, Suttle NF. Some effects of copper deficiency on leucocyte function in sheep and cattle. *Res. Vet. Sci.* 1981; doi:10.1016/s0034-5288(18)32485-8.
19. Crocker A, Lee C, Aboko-Cole G, Durham C. Interaction of nutrition and infection: effect of copper deficiency on resistance to Trypanosoma lewisi. *J Natl Med Assoc* 1992;84(8):697-706.
20. Babu U, Failla ML. Copper status and function of neutrophils are reversibly depressed in marginally and severely copper-deficient rats. *J. Nutr.* 1990; doi:10.1093/jn/120.12.1700.
21. Babu U, Failla ML. Respiratory burst and candidacidal activity of peritoneal macrophages are impaired in copper-deficient rats. *J. Nutr.* 1990; doi:10.1093/jn/120.12.1692.
22. Wagner D, Maser J, Lai B, Cai Z, Barry CE 3rd, Höner Zu Bentrup K, Russell DG, Bermudez LE. Elemental analysis of Mycobacterium avium-, Mycobacterium tuberculosis-, and Mycobacterium smegmatis-containing phagosomes indicates pathogen-induced microenvironments within the host cell's endosomal system. *J Immunol* 2005; Feb 1;174(3):1491-500. doi: 10.4049/jimmunol.174.3.1491.
23. White C, Lee J, Kambe T, Fritsche K, Petris MJ. A role for the ATP7A copper-transporting ATPase in macrophage bactericidal activity. *J. Biol. Chem.* 2009; doi:10.1074/jbc.M109.070201.
24. Samanovic M I, Ding C, Thiele DJ, Darwin KH. Copper in microbial pathogenesis: Meddling with the metal. *Cell Host and Microbe* 2012; doi:10.1016/j.chom. 2012.01.009.
25. Argüello JM, Mandal AK, Mana-Capelli S. Heavy metal transport CPx-ATPases from the thermophile Archaeoglobus fulgidus. *Annals of the New York Academy of Sciences* 2003; doi:10.1111/j.1749-6632.2003.tb07162.x.
26. Arnab Gupta, Svetlana Lutsenko. Evolution of Copper Transporting ATPases in Eukaryotic Organisms. *Curr. Genomics* 2012; doi:10.2174/138920212799860661.
27. Lutsenko S, Barnes NL, Bartee MY, Dmitriev OY. Function and regulation of human copper-transporting ATPases. *Physiological Reviews* 2007; doi:10.1152/physrev. 00004.2006.
28. Banerjee S, Datta R. Leishmania infection triggers hepcidin-mediated proteasomal degradation of Nramp1 to increase phagolysosomal iron availability. *Cell. Microbiol.* 2020; doi:10.1111/cmi.13253.
29. Myler PJ, Audleman L, deVos T, Hixson G, Kiser P, Lemley C, Magness C, Rickel E, Sisk E, Sunkin S, Swartzell S, Westlake T, Bastien P, Fu G, Ivens A, Stuart K. Leishmania major Friedlin chromosome 1 has an unusual distribution of protein-coding genes. *Proc Natl Acad Sci U S A.* 1999; Mar 16;96(6):2902-6. doi: 10.1073/pnas.96.6.2902.
30. Pal DS, Abbasi M, Mondal DK, Varghese BA, Paul R, Singh S, Datta R. Interplay between a

cytosolic and a cell surface carbonic anhydrase in pH homeostasis and acid tolerance of Leishmania. *J Cell Sci*. 2017; Feb 15;130(4):754-766. doi: 10.1242/jcs.199422. Epub 2017 Jn 6.

31. Aslett M, Aurrecoechea C, Berriman M, Brestelli J, Brunk BP, Carrington M, Depledge DP, Fischer S, Gajria B, Gao X, Gardner MJ, Gingle A, Grant G, Harb OS, Heiges M, Hertz-Fowler C, Houston R, Innamorato F, Iodice J, Kissinger JC, Kraemer E, Li W, Logan FJ, Miller JA, Mitra S, Myler PJ, Nayak V, Pennington C, Phan I, Pinney DF, Ramasamy G, Rogers MB, Roos DS, Ross C, Sivam D, Smith DF, Srinivasamoorthy G, Stoeckert CJ Jr, Subramanian S, Thibodeau R, Tivey A, Treatman C, Velarde G, Wang H. TriTrypDB: a functional genomic resource for the Trypanosomatidae. Nucleic Acids Res. 2010; Jan;38(Database issue):D457-62. doi: 10.1093/nar/gkp851. Epub 2009 Oct 20.

32. Krogh A, Larsson B, Von Heijne G, Sonnhammer ELL. Predicting transmembrane protein topology with a hidden Markov model: Application to complete genomes. *J. Mol. Biol.* 2001; doi:10.1006/jmbi.2000.4315.

33. Sievers F, Wilm A, Dineen D, Gibson TJ, Karplus K, Li W, Lopez R, McWilliam H, Remmert M, Söding J, Thompson JD, Higgins DG. Fast, scalable generation of high-quality protein multiple sequence alignments using Clustal Omega. *Mol Syst Biol* 2011; Oct 11;7:539. doi: 10.1038/msb.2011.75.

34. Waterhouse AM, Procter JB, Martin DMA, Clamp M, Barton GJ. Jalview Version 2-A multiple sequence alignment editor and analysis workbench. *Bioinformatics* 2009; doi:10.1093/bioinformatics/btp033.

35. Wilkins MR, Gasteiger E, Bairoch A, Sanchez JC, Williams KL, Appel RD, Hochstrasser DF. Protein identification and analysis tools in the ExPASy server. *Methods Mol Biol* 1999;112:531-52. doi: 10.1385/1-59259-584-7:531.

36. Eswar N, Webb B, Marti-Renom MA, Madhusudhan MS, Eramian D, Shen MY, Pieper U, Sali A. Comparative protein structure modeling using Modeller. *Curr Protoc Bioinformatics* 2006; Oct;Chapter 5:Unit-5.6. doi: 10.1002/0471250953.bi0506s15.

37. Shen M, Sali A. Statistical potential for assessment and prediction of protein structures. *Protein Sci* 2006; doi:10.1110/ps.062416606.

38. Jorgensen WL, Chandrasekhar J, Madura JD, Impey RW, Klein ML. Comparison of simple potential functions for simulating liquid water. *J. Chem. Phys.* 1983; doi:10.1063/1.445869.

39. Bussi G, Zykova-Timan T, Parrinello M. Isothermal-isobaric molecular dynamics using stochastic velocity rescaling. *J Chem Phys* 2009; doi:10.1063/1.3073889.

40. Parrinello M, Rahman A. Polymorphic transitions in single crystals: A new molecular dynamics method. *J. Appl. Phys.* 1981; doi:10.1063/1.328693.

41. Darden T, York D, Pedersen L. Particle mesh Ewald: An N·log(N) method for Ewald sums in large systems. *J. Chem. Phys.* 1993; doi:10.1063/1.464397.

42. Abraham MJ, van der Spoel D, Lindahl E, Hess B and the G. development team. Gromacs 2019.2.

GROMACS User Man. version 2019.

43. Hornak V, Abel R, Okur A, Strockbine B, Roitberg A, Simmerling C. Comparison of multiple Amber force fields and development of improved protein backbone parameters. *Proteins* 2006; Nov 15;65(3):712-25. doi: 10.1002/prot.21123.

44. Gietz RD, Schiestl RH, Willems AR, Woods RA. Studies on the transformation of intact yeast cells by the LiAc/SS-DNA/PEG procedure. *Yeast* 1995; doi:10.1002/yea.320110408.

45. Wickham H. ggplot2: Elegant Graphics for Data Analysis. *Springer-Verlag* New York 2016; ISBN 978-3-319-24277-4.

46. Team R. A language and environment for statistical computing. *Computing* 2006; 1. 10.1890/0012-9658(2002)083[3097:CFHIWS]2.0.CO;2.

47. Dollwet HHA, Sorenson JRJ. Historic uses of copper compounds in medicine. *Trace Elem. Med.* 1985.

48. Isah MB, Goldring JPD, Coetzer THT. Expression and copper binding properties of the N-terminal domain of copper P-type ATPases of African trypanosomes. *Mol. Biochem. Parasito.*. 2020; doi:10.1016/j.molbiopara.2019.111245.

49. Vanderwerf SM, Cooper MJ, Stetsenko IV, Lutsenko S. Copper Specifically Regulates Intracellular Phosphorylation of the Wilson's Disease Protein, a Human Copper-transporting ATPase. *J. Biol. Chem.* 2001; doi:10.1074/jbc.M102055200.

50. Hasan NM, Gupta A, Polishchuk E, Yu CH, Polishchuk R, Dmitriev OY, Lutsenko S. Molecular events initiating exit of a copper-transporting ATPase ATP7B from the trans-Golgi network. *J Biol Chem* 2012; Oct 19;287(43):36041-50. doi: 10.1074/jbc.M112.370403. Epub 2012 Aug 16.

51. Cater MA, Forbes J, La Fontaine S, Cox D, Mercer JFB. Intracellular trafficking of the human Wilson protein: The role of the six N-terminal metal-binding sites. *Biochem. J.* 2004; doi:10.1042/BJ20031804.

52. Chun H, Catterton T, Kim H, Lee J, Kim BE. Organ-specific regulation of ATP7A abundance is coordinated with systemic copper homeostasis. *Sci. Rep.* 2017; doi:10.1038/s41598-017-11961-z.

53. Forbes JR, Cox DW. Functional characterization of missense mutations in ATP7B: Wilson disease mutation or normal variant? *Am. J. Hum. Genet.* 1998; doi:10.1086/302163.

54. Petris MJ, Mercer JF, Culvenor JG, Lockhart P, Gleeson PA, Camakaris J. Ligand-regulated transport of the Menkes copper P-type ATPase efflux pump from the Golgi apparatus to the plasma membrane: a novel mechanism of regulated trafficking. *EMBO J* 1996; Nov 15;15(22):6084-95.

55. Nyasae L, Bustos R, Braiterman L, Eipper B, Hubbard A. Dynamics of endogenous ATP7A (Menkes protein) in intestinal epithelial cells: Copper-dependent redistribution between two intracellular sites. *Am. J. Physiol. - Gastrointest. Liver Physiol.* 2007; doi:10.1152/ajpgi.00472.2006.

56. Pase L, Voskoboinik I, Greenough M, Camakaris J. Copper stimulates trafficking of a distinct pool of the Menkes copper ATPase (ATP7A) to the plasma membrane and diverts it into a rapid recycling

pool. *Biochem. J.* 2004; doi:10.1042/BJ20031181.

57. Lively CM. Antagonistic Coevolution and Sex. *Evol. Educ. Outreach* 2010; doi:10.1007/s12052-009-0196-2.

58. Thomas CA, Li Y, Kodama T, Suzuki H, Silverstein SC, El Khoury J. Protection from lethal gram-positive infection by macrophage scavenger receptor-dependent phagocytosis. *J Exp Med* 2000; Jan 3;191(1):147-56. doi: 10.1084/jem.191.1.147.

59. Mackie J, Szabo EK, Urgast DS, Ballou ER, Childers DS, MacCallum DM, Feldmann J, Brown AJ. Host-Imposed Copper Poisoning Impacts Fungal Micronutrient Acquisition during Systemic Candida albicans Infections. *PLoS One* 2016; Jun 30;11(6):e0158683. doi: 10.1371/journal.pone.0158683.

60. Dey R, Meneses C, Salotra P, Kamhawi S, Nakhasi HL, Duncan R. Characterization of a Leishmania stage-specific mitochondrial membrane protein that enhances the activity of cytochrome c oxidase and its role in virulence. *Mol Microbiol* 2010;77(2):399-414. doi:10.1111/j.1365-2958.2010.07214.x

61. Polishchuk EV, Concilli M, Iacobacci S, Chesi G, Pastore N, Piccolo P, Paladino S, Baldantoni D, van IJzendoorn SC, Chan J, Chang CJ, Amoresano A, Pane F, Pucci P, Tarallo A, Parenti G, Brunetti-Pierri N, Settembre C, Ballabio A, Polishchuk RS. Wilson disease protein ATP7B utilizes lysosomal exocytosis to maintain copper homeostasis. *Dev Cell* 2014; Jun 23;29(6):686-700. doi: 10.1016/j.devcel.2014.04.033. Epub 2014 Jun 5.

62. Das S, Maji S, Ruturaj, Bhattacharya I, Saha T, Naskar N, Gupta A. Retromer retrieves the Wilson disease protein ATP7B from endolysosomes in a copper-dependent manner. *J Cell Sci* 2020; Dec 24;133(24):jcs246819. doi: 10.1242/jcs.246819.

63. Kenthirapalan S, Waters AP, Matuschewski K, Kooij TWA. Copper-transporting ATPase is important for malaria parasite fertility. *Mol. Microbiol.* 2014; doi:10.1111/mmi.12461.

64. McConville MJ, de Souza D, Saunders E, Likic VA, Naderer T. Living in a phagolysosome; metabolism of Leishmania amastigotes. *Trends in Parasitology* 2007; doi:10.1016/j.pt.2007.06.009.

65. Achard ME, Stafford SL, Bokil NJ, Chartres J, Bernhardt PV, Schembri MA, Sweet MJ, McEwan AG. Copper redistribution in murine macrophages in response to Salmonella infection. *Biochem J* 2012; May 15;444(1):51-7. doi: 10.1042/BJ20112180.

66. Parmar P, Limson J, Nyokong T, Daya S. Melatonin protects against copper-mediated free radical damage. *J. Pineal Res.* 2002; doi:10.1034/j.1600-079X.2002.01859.x.

Legends to figures

Fig1. Survivability and growth of wild-type *L. major* promastigotes and amastigotes at increasing copper concentration (A) Wild-type (WT) promastigote count in copper range between 0-500µM and 24h post-incubation. Bars represent the cell count after 24 hrs of growth (First grey bar represents initial seeded number of promastigotes). Error bars represent mean ± SD of values from 3 independent experiments. * indicate significance of difference in number of promastigotes growing without copper supplementation with respect to those growing under external copper condition. **P<0.01, ***P<0.001, ****P<0.0001; (Student's t-test). **(B)** J774A.1 macrophages infected with WT *L. major*. Bars represent amastigote count inside the macrophage at different copper levels. Error bars represent mean ± SD of values from 3 independent experiments. * represents significance of difference in number of amastigotes surviving inside macrophages without any external copper supplementation with respect to those surviving inside macrophages under external copper condition. **P<0.01, ****P<0.0001

Fig2. Characterization of LmATP7 (A) Schematic representation of the putative Leishmanial copper transporting P-type ATPase comprising of the three N-terminal metal binding (M1, M2 and M3), nine transmembrane (numbered 1–9), E1-E2 ATPase and hydrolase domains. **(B)** Amino acid sequence alignment of the putative Leishmanial copper transporting P-type ATPase (accession number: XP_001685970.1) with copper transporting P-type ATPases from *Trypanosoma cruzi* (XP_810568.1), *Pseudomonas putida* (AAP88295.1), *Saccharomyces cerevisiae* (AJU90155.1), *Drosophila melanogaster* (NP_001259466.1), *Danio rerio* (NP_001036185.1), *Mus musculus* (AAA57445.1), *Homo sapiens* (AAA35580.1). Conserved CXXC motifs in the N-terminal domain, actuator (A) domain TGE loop, DKTGT motif in the phosphorylation (P) domain, TGDN and GXGXND and SXHP motifs in the nucleotide (N) domain ATP-binding site are highlighted. Conserved CPC, YNXXXXP and MXXSS motifs are highlighted in the predicted seventh, eighth and ninth transmembrane domains respectively. **(C)** Agarose gel electrophoresis showing amplification of *LmATP7* gene and its transcriptional expression as indicated by 3.5 kb PCR products amplified from both total genomic DNA (left image) and cDNA (reverse transcribed from mRNA) (right image) **(D)** Homology model of N-terminal copper binding domains of LmATP7. (a) Modelled structure of HM1 domain (yellow) with “CRGC” motif shown in inset. (b) Modelled structure of HM2 domain (green) with “CTSC” motif shown in inset. (c) Modelled structure of HM3 domain (blue) with “CASC” motif shown in inset. (d) Modelled structure of Hm2 and HM3 domains combined together (red). (e) Superposition of the individual Hm2 (green) and HM3 (blue) domains on the combined model (red).

Fig3. Intracellular localization and expression of LmATP7 (A) *L. major* promastigotes stably expressing LmATP7 as a C-terminal GFP-tagged protein (LmATP7–GFP) (right column) or not (left column) were immunostained with antibodies against GFP (green). Promastigote nuclei is stained with DAPI (Blue) **(B)** *L. major* cells stably expressing LmATP7–GFP were co-stained for GFP (green) and LmCA2 (Carbonic

anhydrase 2) (red). The merged images show colocalization of proteins (yellow). DAPI (blue) was used to stain the nucleus. Scale bar: 5 µm. **(C)** Pearson's correlation coefficient of colocalization (PCC) between GFP-LmATP7 and LmCA2 represented by a box plot. The number of *Leishmania* amastigotes counted to obtain the data is denoted by 'n'. **(D)** Immunoblot showing HEK293T expressing GFP-LmATP7. GAPDH is used as a loading control (lower panel). **(E)** HEK293T cells expressing GFP-LmATP7 (green) co-stained for Golgin97 (red) and calnexin (blue) under basal (top row) and copper treated (50µM for 2 hrs) (bottom row). The merged images show GFP-LmATP7 colocalization with Golgin97 as indicted by arrowheads. Vesicles are labelled with arrows (bottom row). Scale bar: 5 µm.

Fig4. LmATP7 transports copper (A) Bar diagram showing *LmATP7* transcript level normalized against *rRNA45* in basal (left) and 50µM, 2 hr, copper treated (right) *L. major*. Error bars represent mean ± SD of values calculated from 3 independent experiments. * indicate significant difference with respect to the *LmATP7* transcript level. ****P≤0.0001. **(B)** Complementation of ccc2 mutant yeast by LmATP7. Wild-type (Wt) and deletion (ccc2) yeast strains were transformed with constructs mentioned within the parentheses. Dilution spotting was performed on SD-Ura plate (Control) and 250µM ferrozine treated SD-Ura plate (Iron-limited) with yeast transformants (OD_{600} = 0.2, 0.02, 0.002, 0.0002). Images of the plates were taken after 3 days of incubation at 30°C.

Fig5. LmATP7 overexpression in promastigotes imparts copper resistant (A) Bar diagram showing *LmATP7* transcript level normalized against *rRNA45* in LmATP7 overexpressing (OE) *L. major* (right bar) or not (left bar). Error bars represent mean ± SD of values calculated from 3 independent experiments. * indicate significance of difference with respect to the *LmATP7* transcript level **P≤0.01(Student's t-test). **(B)** Promastigote count at of Wild-type (WT; grey bar), vector control (Control; striped bar) and LmATP7 overexpressed (LmATP7; black bar) grown in medium containing copper in a range between 0-500µM for 24hrs. First group of bars represent initial seeded number of promastigotes. Error bars represent mean ± SD of values from 3 independent experiments. * indicate significance of difference in number of wild-type promastigotes with respect to number of vector control and LmATP7 overexpressed promastigotes at a particular external copper concentration. *P≤0.05, **P<0.01, ***P<0.001, ****P<0.0001, n.s: non-significant.

Fig6. *Leishmania* infection elicits a host response that is mediated through its copper homeostasis genes (A) J774A.1 macrophage cells were either infected or not with *L. major* promastigotes for 12 hrs and 30 hrs. Bar diagram shows transcript levels of macrophagic copper homeostasis genes *ATP7A*, *CTR1*, *CTR2*, and *ATOX1* normalized against *β-Actin* mRNA levels. Error bars represent mean ± SD of values calculated from 3 independent experiments. *indicate significance in difference in the transcript level of the genes between infected macrophages with respect to those in uninfected macrophages at the particular time points,

(12 hrs, 30 hrs). *P≤0.05, **P<0.01, n.s : non-significant. **(B)** J774A.1 macrophages were infected with *L. major* promastigotes and stained with anti-ATP7A (green) and anti-Rab11 (red) or anti-Rab7 (red) or anti-Lamp1 (red) or anti-Lamp2 (red) at 24 hrs post infection. The merged images represent colocalization of ATP7A with *Leishmania* amastigote nuclei (blue) and endosomal markers (Rab11, Rab7, Lamp1, Lamp2) (red). Both macrophage and *Leishmania* nuclei were stained with DAPI (blue). White arrows indicates intracellular parasites in infected cells (smaller nuclei). The magnified inset corresponds to the region of the merged image marked by arrowheads indicating the association of ATP7A and endosomal markers with *Leishmania* positive endosomes. Scale bar: 5µm. **(C)** Bar plot (mean ± SD) representing relative *Leishmania* amastigote nuclei (N) localization with only ATP7A (7A + N), only endosomal markers (Endosome + N) and with both ATP7A and endosomal markers (7A + Endosome + N). The number of *Leishmania* nuclei counted to obtain the data for each condition are 197, 189, 274, 243 (for Rab11, Rab7, Lamp1, Lamp2 respectively) from three independent experiments. Error bars represent mean ± SD of values calculated from 3 independent experiments.

Fig7. (A) Epifluorescence microscopy images showing J774A.1 macrophages infected with wild-type (WT;), vector control (Control) and LmATP7 overexpressed (LmATP7) *L. major* strains as indicated by large macrophage nuclei surrounded by smaller *Leishmania* amastigote nuclei stained with DAPI after 24 hrs post infection **(B)** Graphical representation of amastigotes in macrophages infected with wild-type (WT; grey bar), vector control (Control; striped bar) and LmATP7 overexpressed (LmATP7; black bar) *L. major* strains and treated with copper or not for 24 hrs. Nuclei were stained with DAPI. Error bars represent mean ± SD of values from 3 independent experiments. * indicate significance of difference in number of wild-type amastigotes surviving inside macrophages with respect to number of vector control and LmATP7 overexpressed amastigotes surviving inside macrophages at a particular copper concentration *P≤0.05, **P<0.01, ***P<0.001, ****P<0.0001; (Student's t-test).

Fig8. Proposed model describing the role of parasite and host copper P-type ATPases in *Leishmania* infection Macrophages channelize copper via ATP7A trafficking from Golgi to the *Leishmania* positive endo/lysosomal compartments. *Leishmania* amastigotes, in turn, export copper via LmATP7 to reduce the host-mediated copper stress in order to thrive within the host as indicated by black double headed arrows. Orange arrows indicate the endolysosomal pathway followed by amastigote after its entry into the macrophage.

Supplementary figs:

S1. Homology model of the Copper binding motifs of LmATP7 protein (a1) Sequence comparison between HM1 and 1OPZ_A chain with the conserved residues being indicated by "*" symbol. **(a2)** DOPE-per-residue score versus Alignment Position plotted for HM1 (model) and template (1OPZ.pdb). **(b1)** Sequence comparison between combined HM2 and HM3 and 1P6T_A chain with the conserved residues being indicated by "*" symbol. **(b2)** DOPE per residue score versus Alignment Position plotted for HM2_HM3 (model) and template (1P6T.pdb)(c1) Sequence comparison between combined HM2 and 2ROP_A chain with the conserved residues being indicated by "*" symbol. **(c2, c3)** DOPE per residue score versus Alignment Position plotted for HM2 (model) and template **(b)** 2ROP.pdb) and **(c)** 1OPZ.pdb). The third plot shows, with the template corresponding to *B. subtilis* CopA shows clear mismatch between the template and model while the second plot with the template corresponding to metal binding domain 4 of ATP7B shows a greater match. **(d1)** Sequence comparison between combined HM3 and 1YJV_A chain with the conserved residues being indicated by "*" symbol. **(d2,d3)** DOPE per residue score versus Alignment Position plotted for HM3 (model) and template **(b)** 1YJV.pdb) and **(c)** 1OPZ.pdb). The third plot shows, with the template corresponding to *B. subtilis* CopA shows clear mismatch between the template and model while the second plot with the template corresponding to metal binding domain 6 of ATP7A shows a greater match.

S2. Schematic representation of generating C-terminal GFP construct of LmATP7 in *Leishmania* expression vector followed by transfection into wild-type promastigotes to generate LmATP7 overexpressing *L. major* strain.

S3. Macrophage ATP7A traffics upon copper and LPS treatment Control (*left image*), LPS treated (24 hrs) (*middle*) and copper treated (50µM; 2 hrs) (*right*) macrophages immunostained with anti-ATP7A (green). Representative confocal microscopy images represent the localization of ATP7A (green) under copper and LPS treatments. Nuclei were stained with DAPI (blue). Scale bar: 5µm.

S4. LmATP7 overexpression rescues amastigote survivability under copper stress Representative epifluorescence microscopy images showing J774A.1 macrophage infected with wild-type (WT), vector control (Control) and LmATP7 overexpressed (LmATP7) *L. major* strains under a range of external copper concentrations (50-500µM) as indicated by large macrophage nuclei surrounded by smaller *Leishmania* amastigote nuclei. Both nuclei are stained with DAPI after 24 hrs post infection and imaged using Olympus IX-81 epifluorescence microscope.

Figure1.

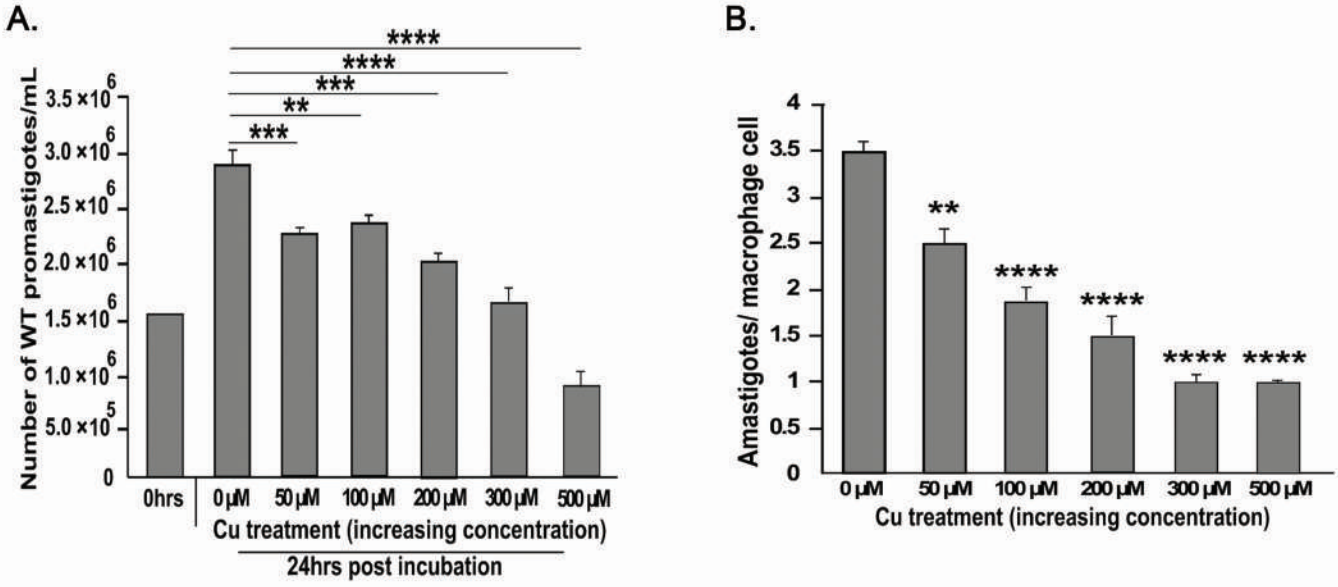
A.
Number of WT promastigotes/mL
3.5 ×10^6
3.0 ×10^6
2.5 ×10^6
2.0 ×10^6
1.5 ×10^6
1.0 ×10^6
5.0 ×10^5
0
****
****
***
**
***
0hrs
0 µM
50 µM
100 µM
200 µM
300 µM
500 µM
Cu treatment (increasing concentration)
24hrs post incubation
B.
Amastigotes/ macrophage cell
4
3.5
3
2.5
2
1.5
1
0.5
0
**
****
****
****
****
0 µM
50 µM
100 µM
200 µM
300 µM
500 µM
Cu treatment (increasing concentration)

Figure2.

A.

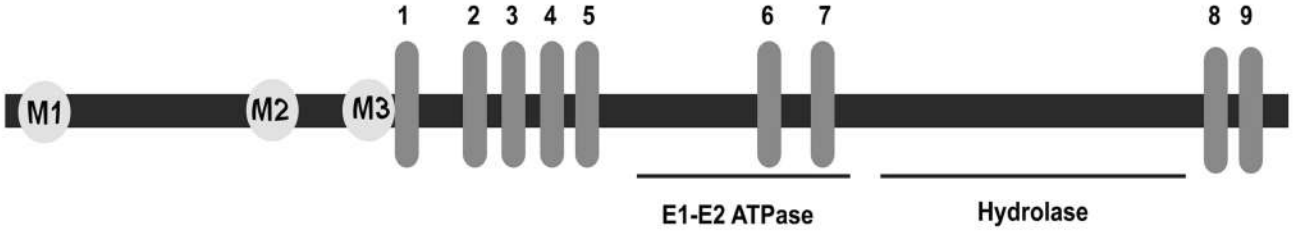

B.

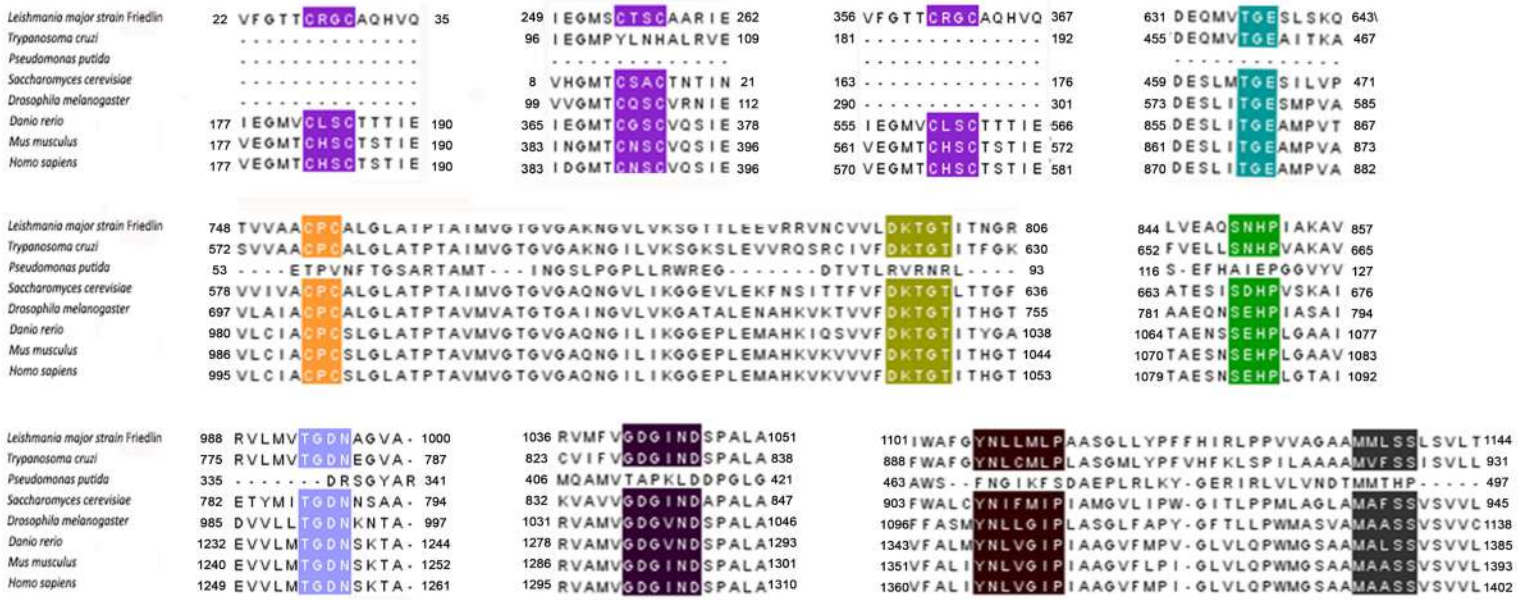

C.

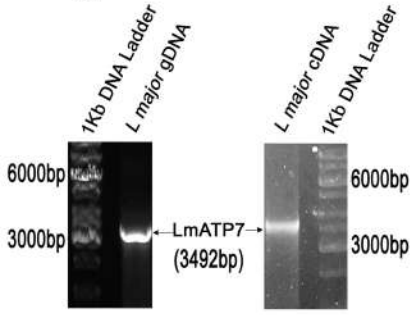

D.

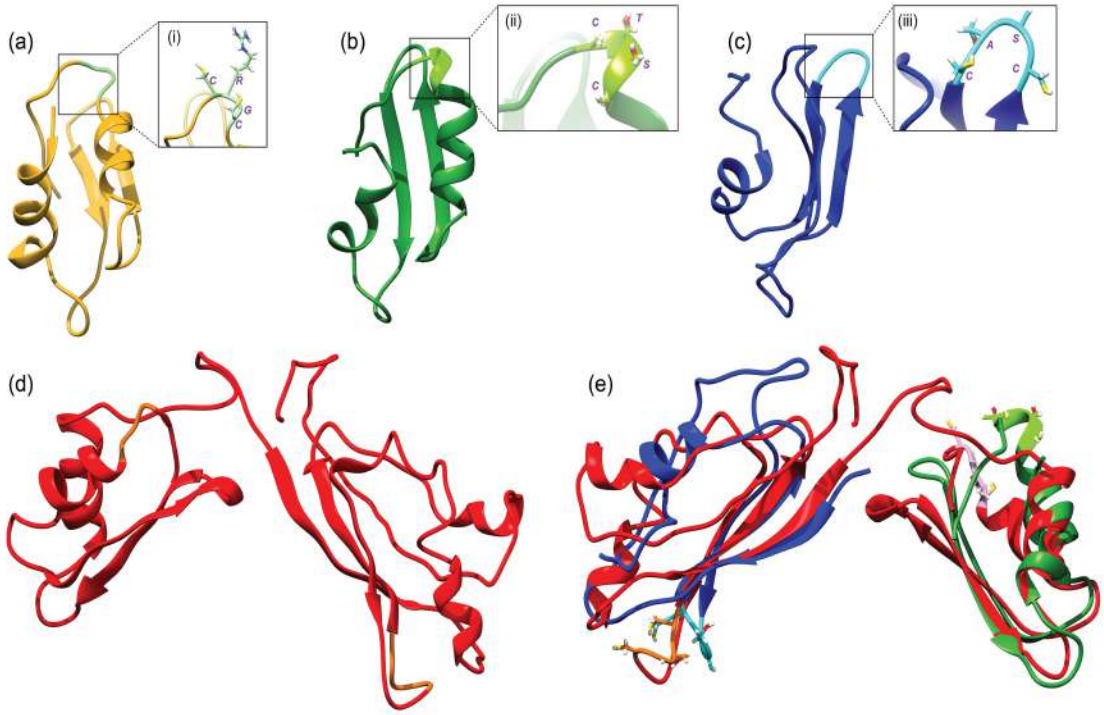

Figure3.

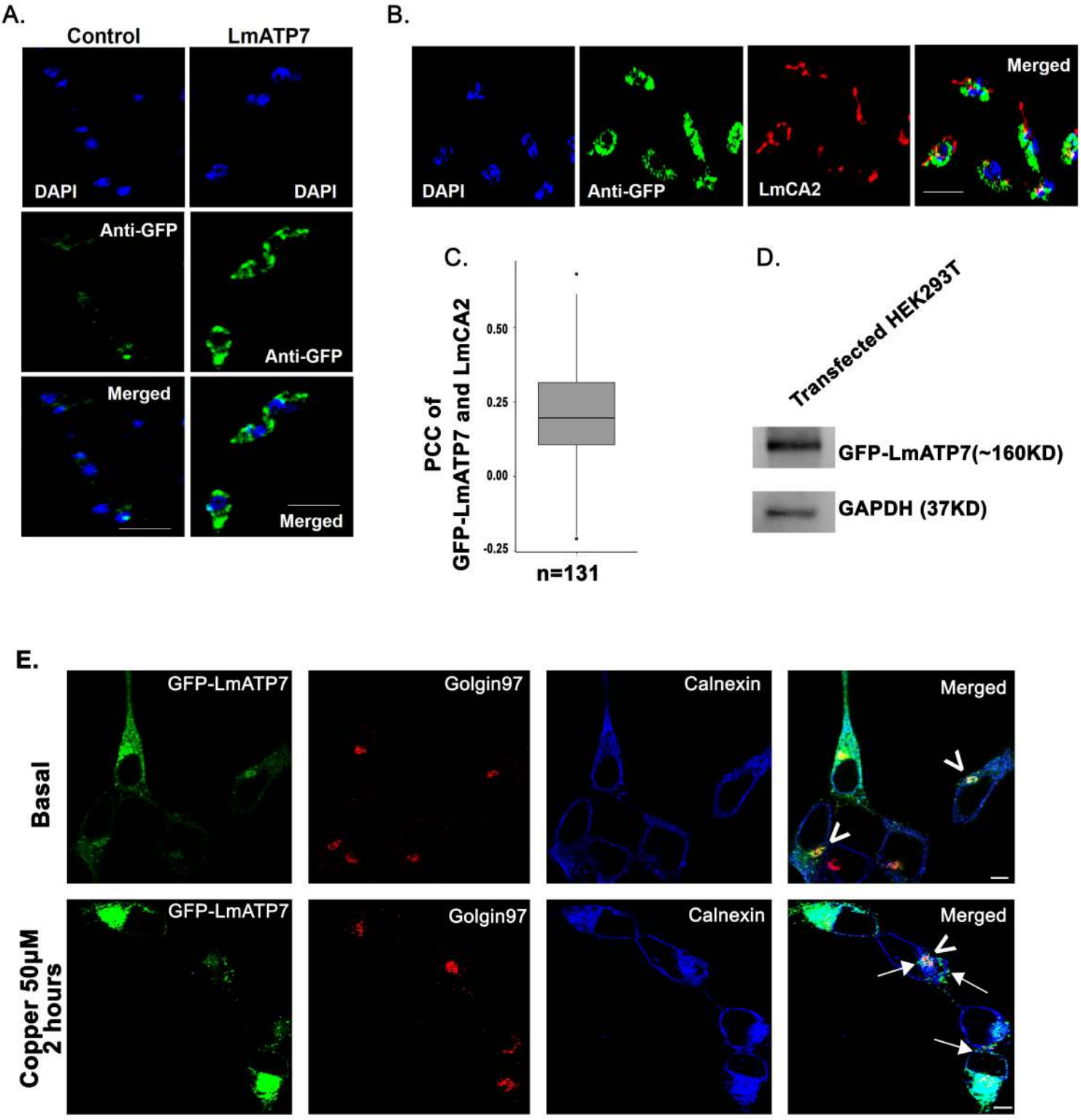
A.
Control
LmATP7
DAPI
DAPI
Anti-GFP
Anti-GFP
Merged
Merged
B.
DAPI
Anti-GFP
LmCA2
Merged
C.
PCC of GFP-LmATP7 and LmCA2
0.50
0.25
0.00
-0.25
n=131
D.
Transfected HEK293T
GFP-LmATP7(~160KD)
GAPDH (37KD)
E.
Basal
Copper 50μM 2 hours
GFP-LmATP7
Golgin97
Calnexin
Merged

Figure4.

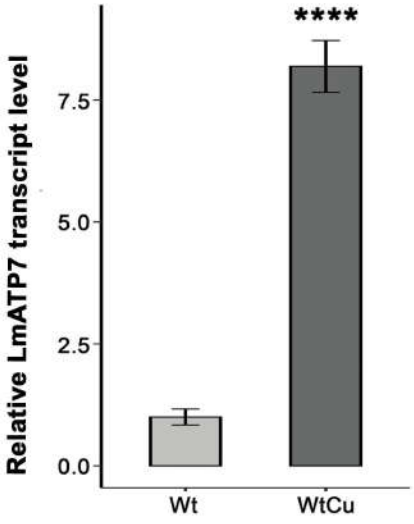
A.
****
Relative LmATP7 transcript level
7.5
5.0
2.5
0.0
Wt
WtCu

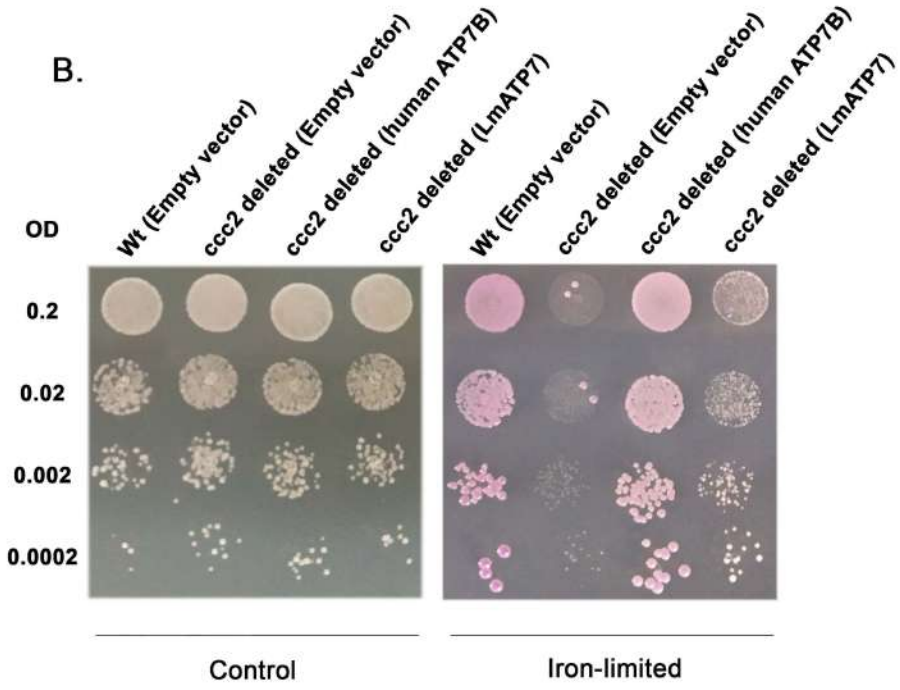
B.
Wt (Empty vector)
ccc2 deleted (Empty vector)
ccc2 deleted (human ATP7B)
ccc2 deleted (LmATP7)
Wt (Empty vector)
ccc2 deleted (Empty vector)
ccc2 deleted (human ATP7B)
ccc2 deleted (LmATP7)
OD
0.2
0.02
0.002
0.0002
Control
Iron-limited

Figure5.

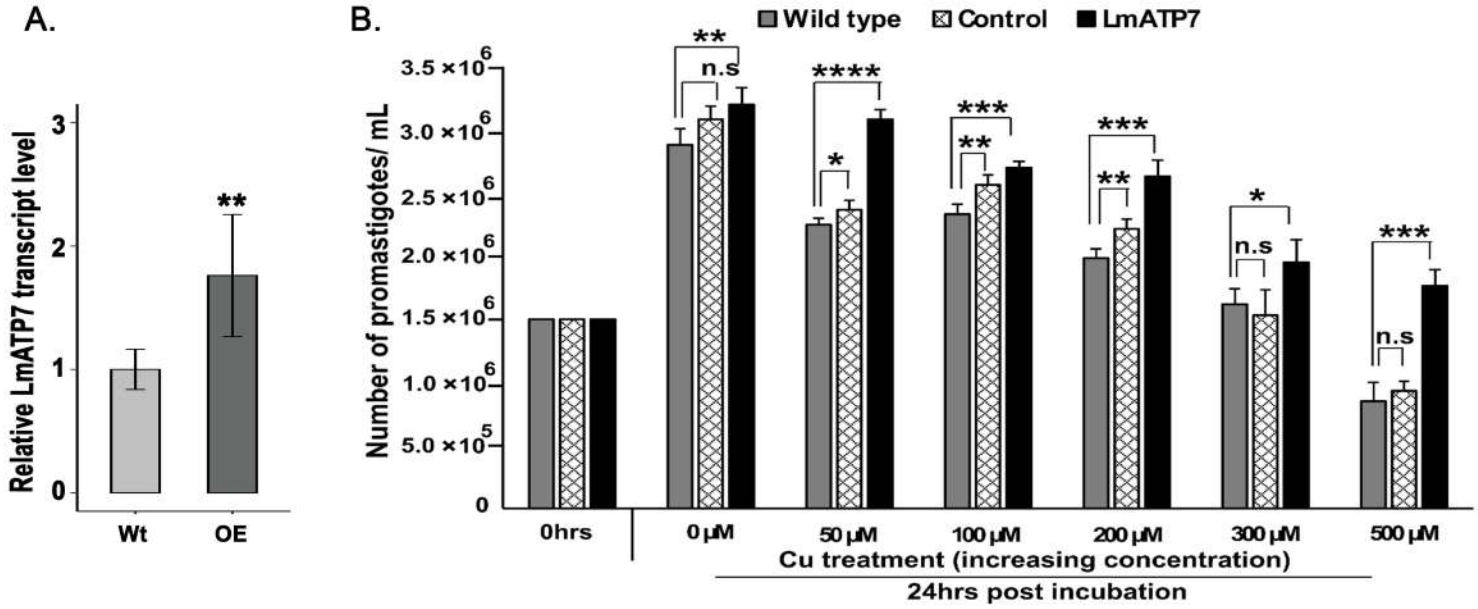
A.
Relative LmATP7 transcript level
3
2
1
0
**
Wt
OE
B.
Wild type
Control
LmATP7
Number of promastigotes/ mL
3.5 ×10^6
3.0 ×10^6
2.5 ×10^6
2.0 ×10^6
1.5 ×10^6
1.0 ×10^6
5.0 ×10^5
0
**
n.s
****
*
***
**
***
**
*
n.s
***
n.s
0hrs
0 µM
50 µM
100 µM
200 µM
300 µM
500 µM
Cu treatment (increasing concentration)
24hrs post incubation

Figure6.

A.

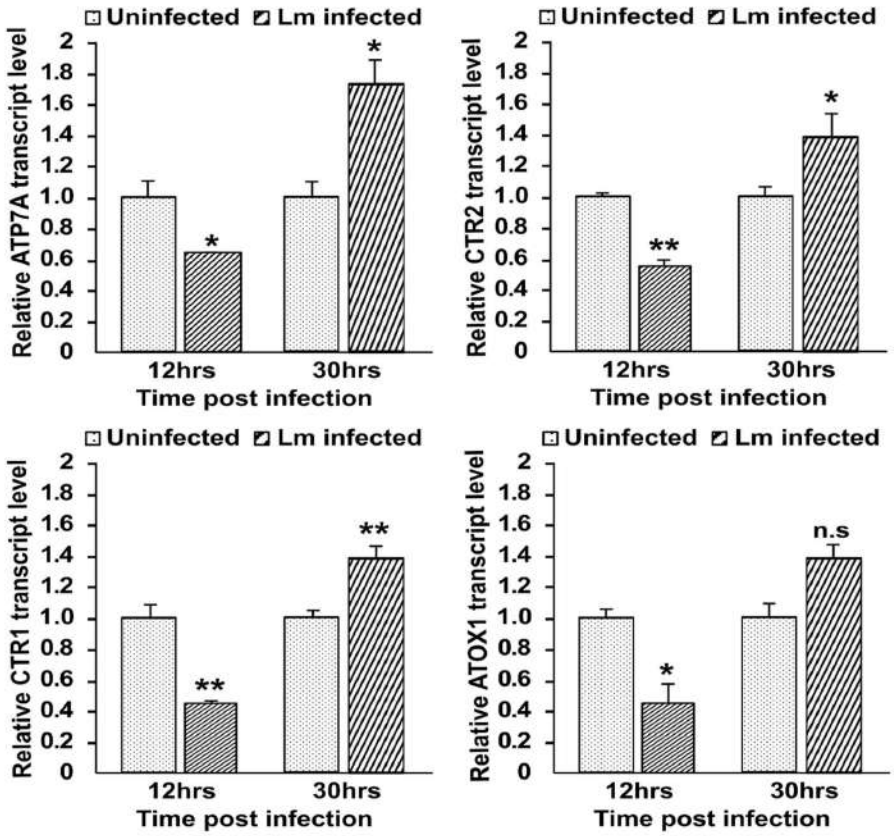
Uninfected
Lm infected
Relative ATP7A transcript level
Relative CTR2 transcript level
Relative CTR1 transcript level
Relative ATOX1 transcript level
12hrs
30hrs
Time post infection
n.s

C.

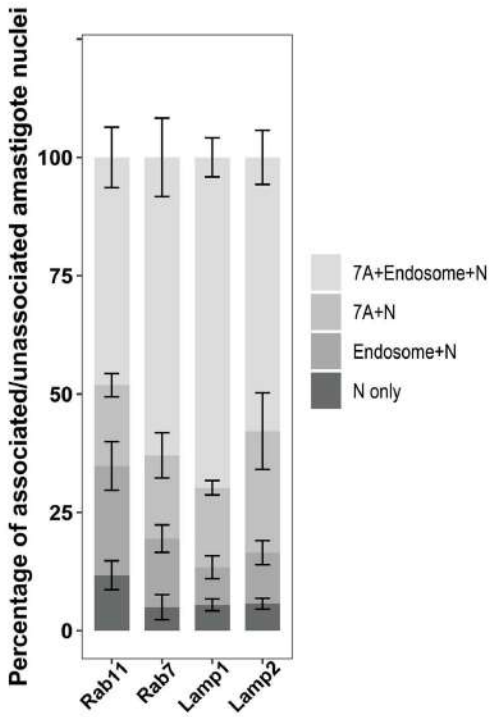
Percentage of associated/unassociated amastigote nuclei
7A+Endosome+N
7A+N
Endosome+N
N only
Rab11
Rab7
Lamp1
Lamp2

B.

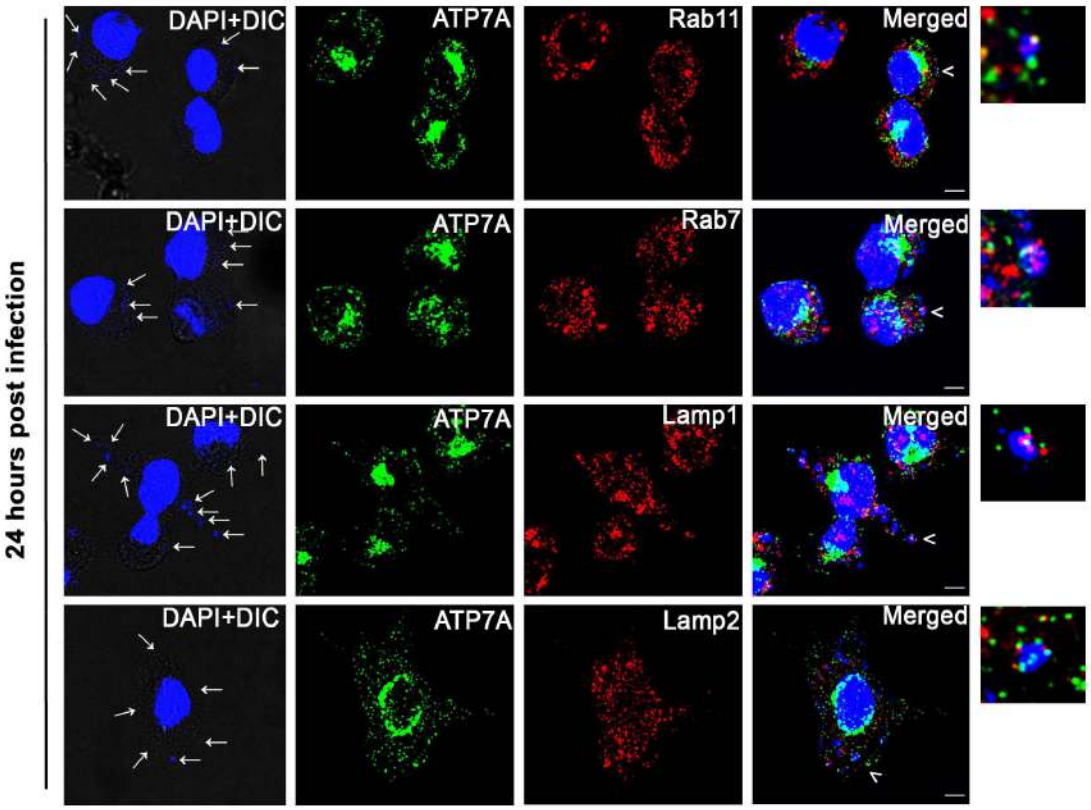
24 hours post infection
DAPI+DIC
ATP7A
Rab11
Rab7
Lamp1
Lamp2
Merged

Figure7.

A.

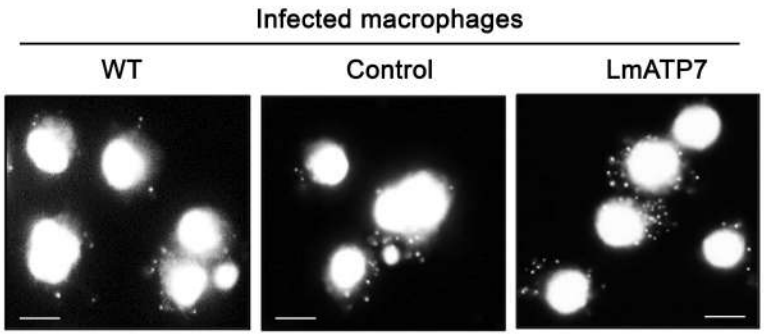
Infected macrophages
WT
Control
LmATP7

B.

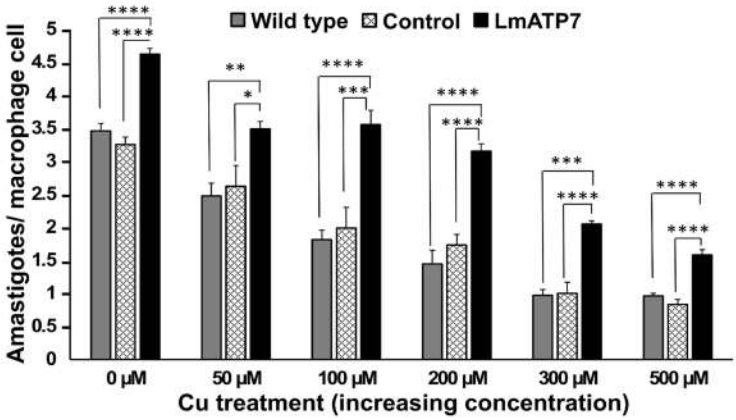
Wild type
Control
LmATP7
Amastigotes/ macrophage cell
0
0.5
1
1.5
2
2.5
3
3.5
4
4.5
5
****
****
**
*
****
***
****
****
***
****
****
****
0 µM
50 µM
100 µM
200 µM
300 µM
500 µM
Cu treatment (increasing concentration)

Figure8.

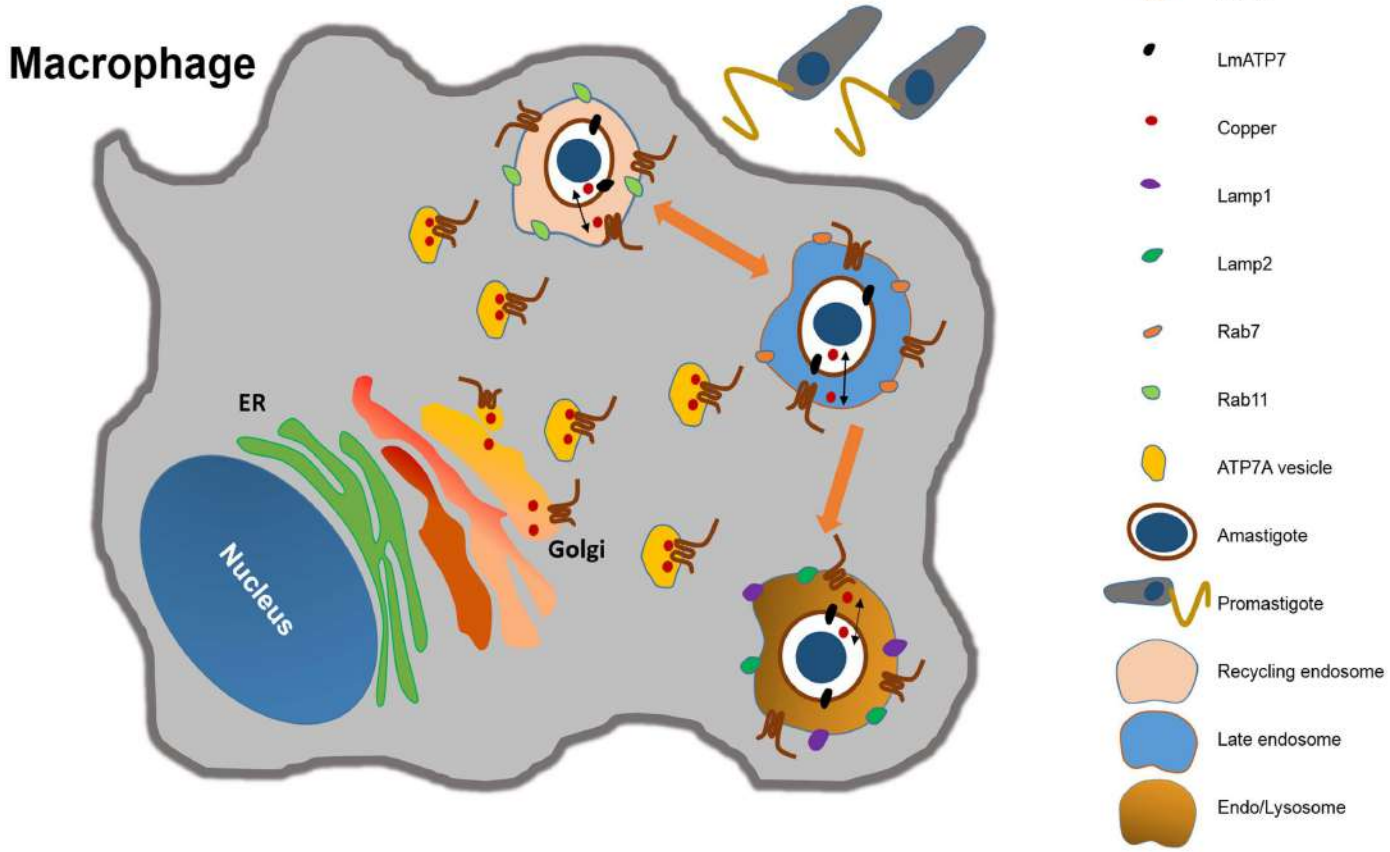
Macrophage
ER
Nucleus
Golgi
ATP7A
LmATP7
Copper
Lamp1
Lamp2
Rab7
Rab11
ATP7A vesicle
Amastigote
Promastigote
Recycling endosome
Late endosome
Endo/Lysosome

S1.

a1

```
 _aln.pos         10        20        30        40        50        60
1opzA     MLSEQKEIAMQVSGMTCAACAARIEKGLKRMPGVTDANVNLATETVNVIYDPAETGT-AAIQEKIEKL
HM1       --------TLNVFGTTCRGCAQHVQENLMTLEGVHSVSVDLDAQLAEVDVDATDAATEFRIEKKMVSM
 _consrvd            * * **  **      *    **    * *      *  *     *   *  *

 _aln.p   70
1opzA     GYHVVIEGR
HM1       GY-------
 _consrvd **
```

a2

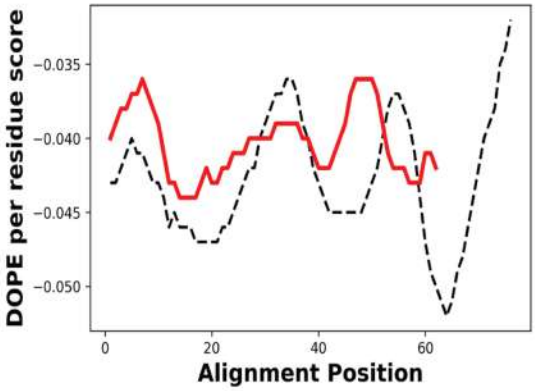

b1

```
 _aln.pos         10        20        30        40        50        60
1p6tA     MLSEQKEIAMQVSGMTCAACAARIEKGLKRMPGVTDANVNLATETVNVIYDPAETGTAAIQEKIEKLG
HM2_HM3   ---------LLIEGMSCTSCAARIEAKLKQLKGVLGASVNFSAMSGQVLHNPALAPLPKVVSCVADMS
 _consrvd              ** *  ******  **   **  * **       *   **

 _aln.p   70        80        90       100       110       120       130
1p6tA     YHVV---------TEKAEFDIEGM-TCAACANRIEKRLNKI-EGVANAPVNF----ALETVTVEYNPK
HM2_HM3   YIVTAQDTTAPLGTADGEQPQEGECKCPTNLQAVPVHVGSVMSGYEHRLVVLGMSCASCAARIEHRLR
 _consrvd * *          *   *   **   *                *     *      *      *

 _aln.pos  140       150       160       170
1p6tA     EASVSDLKEAVDKL-GYKLKLK----GEQDS---IE--GR
HM2_HM3   QMP-TVLNCTVSFVTGTAVITTCTPSGFTDACRMVRSMGY
 _consrvd       *   *    *          *  *        *
```

b2

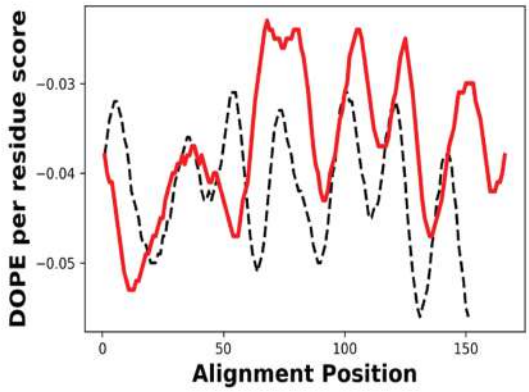

c1

```
 _aln.pos         10        20        30        40        50        60
2rop      VTLQLRIDGMHCKSCVLNIEENIGQLLGVQSIQVSLENKTAQVKYDPSCTSPVALQRAIEALPPGNFK
HM2       ------------------------------------------------------------------
_consrvd

 _aln.p   70        80        90       100       110       120       130
2rop      VSLTCSTTLIAIAGMTCASCVHSIEGMISQLEGVQQISVSLAEGTATVLYNPAVISPEELRAAIEDMG
HM2       ---------LLIEGMSCTSCAARIEAKLKQLKGVLGASVNFSAMSGQVLHNPALAPLPKVVSCVADMS
_consrvd             * ** * **   **    ** **   **        ** ***           **

 _aln.pos  140
2rop      FEASVV
HM2       ------
_consrvd
```

c2

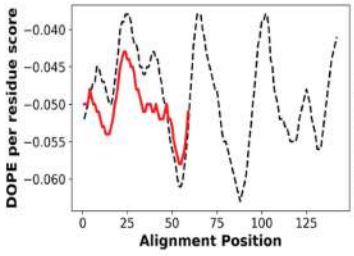

c3

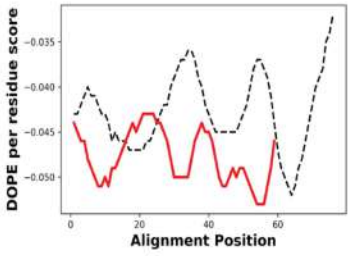

d1

```
 _aln.pos         10        20        30        40        50        60
1yjvA     MGDGVLELVVR-GMTCASCVHKIESSLTK--HRGILYCSVALATNKAHIKYDPEIIGPRDIIHTIESL
HM3       DGEQPQEGECKCPTNLQAVPVHVGSVMSGYEHR-LVVLGMSCASCAARIEHRLRQM-PTVLNCTV-SF
 _consrvd  *    *                 *      **         *   * *        *     *  *

 _aln.p   70
1yjvA     GFEASLVKIE
HM3       -VTGTAV---
 _consrvd       *
```

d2

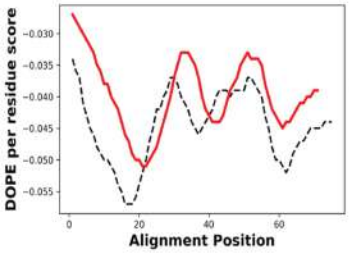

d3

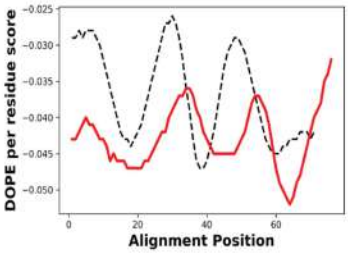

S2.

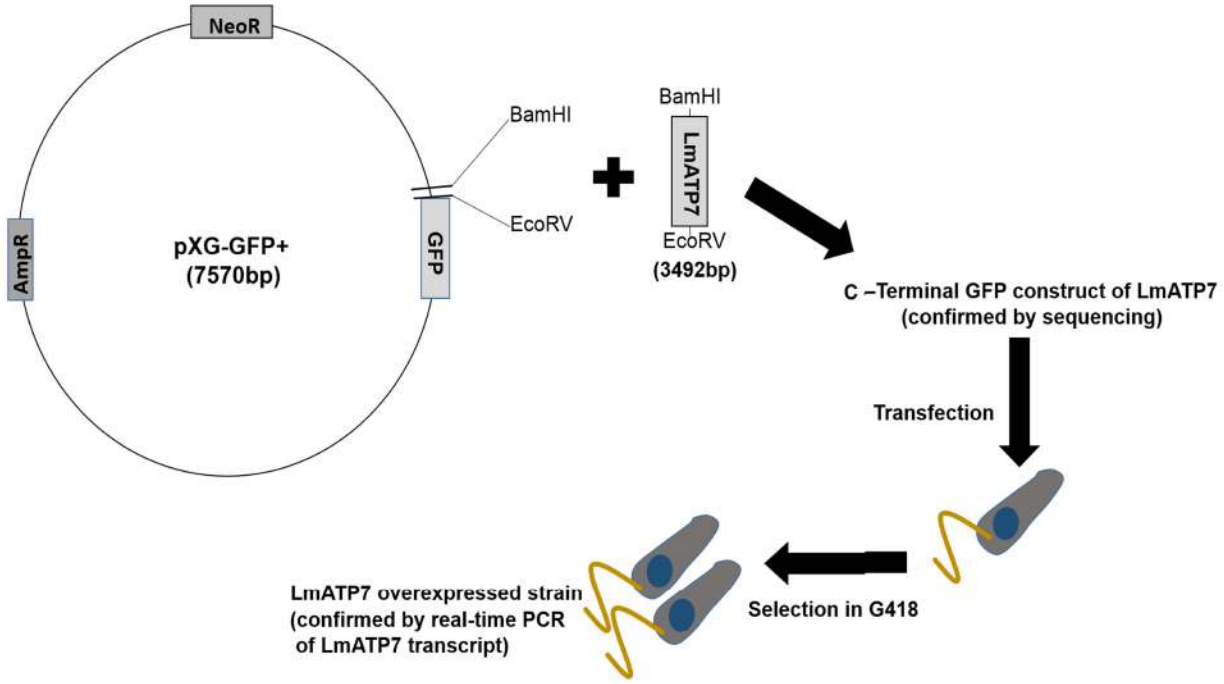
NeoR
AmpR
pXG-GFP+
(7570bp)
GFP
BamHI
EcoRV
BamHI
LmATP7
EcoRV
(3492bp)
C –Terminal GFP construct of LmATP7
(confirmed by sequencing)
Transfection
Selection in G418
LmATP7 overexpressed strain
(confirmed by real-time PCR
of LmATP7 transcript)

S3.

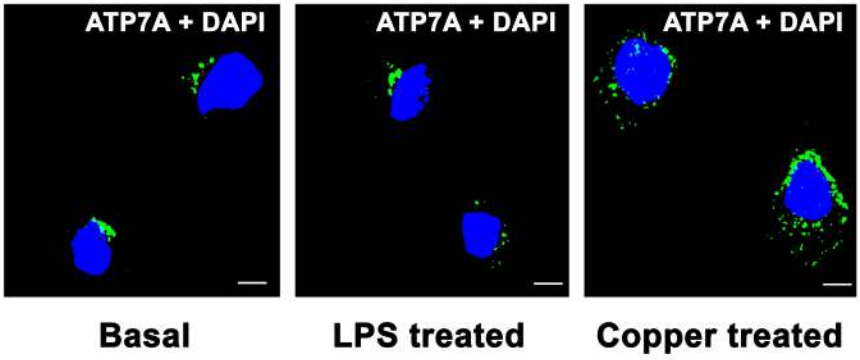
ATP7A + DAPI
ATP7A + DAPI
ATP7A + DAPI
Basal
LPS treated
Copper treated

S4.

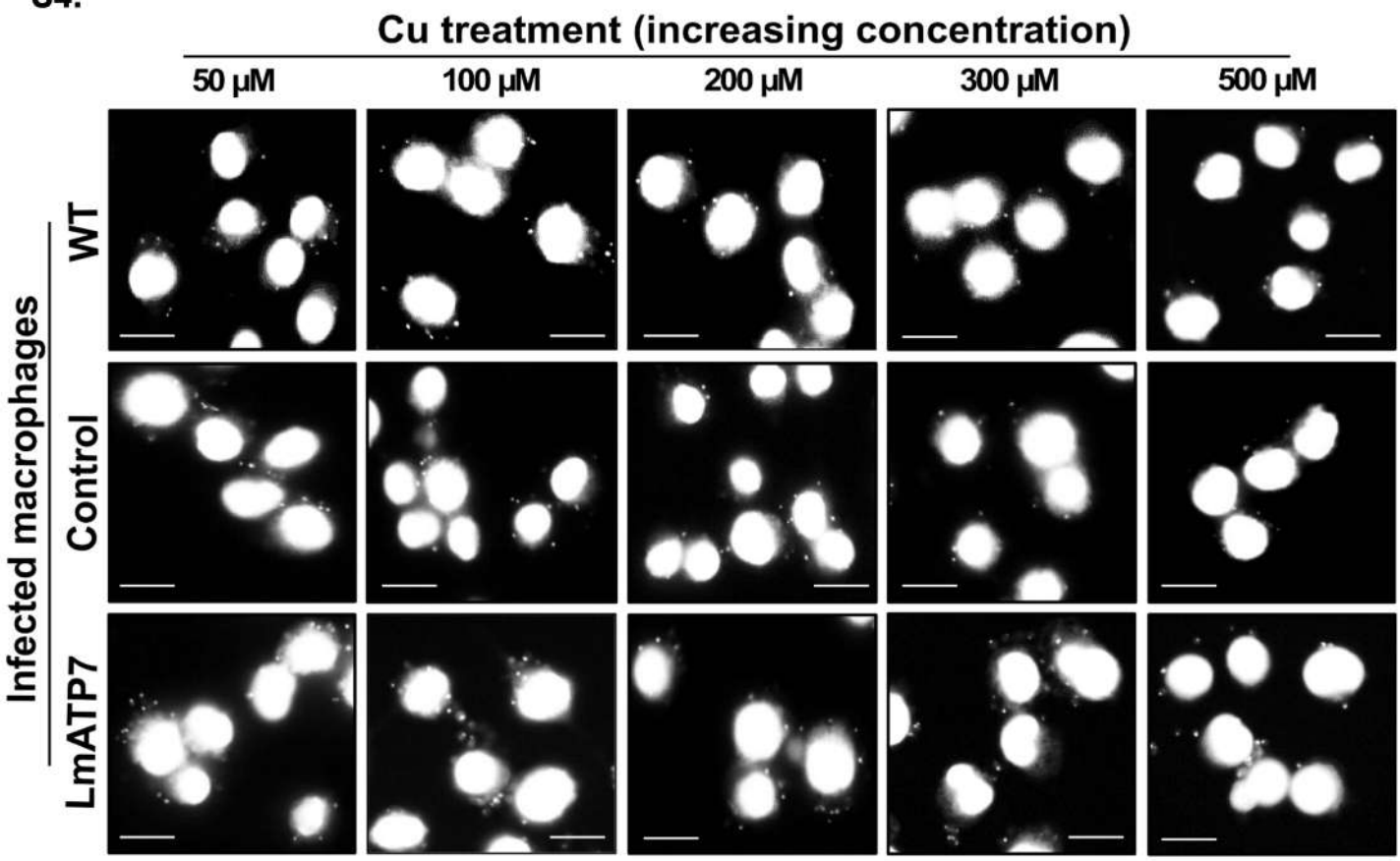
Cu treatment (increasing concentration)
50 µM
100 µM
200 µM
300 µM
500 µM
Infected macrophages
WT
Control
LmATP7